THE UNIVERSITY OF MICHIGAN

COLLEGE OF LITERATURE, SCIENCE, AND THE ARTS
Department of Physics

Final Report

INFRARED STUDIES:
INTERFEROMETRY
DERIVATIVE ABSORPTION SPECTROSCOPY
FAR-INFRARED SPECTRUM OF H_2O_2
ELECTRIC FIELD INDUCED ABSORPTION IN H_2 AND D_2
STARK EFFECTS IN HCN, CH_3F, NH_3, AND H_2O

Charles H. Church
Robert Hunt
Paul Maker
C. W. Peters

UMRI Project 2609

under contract with:

UNITED STATES AIR FORCE
AIR RESEARCH AND DEVELOPMENT COMMAND
AIR FORCE CAMBRIDGE RESEARCH CENTER
GEOPHYSICS RESEARCH DIRECTORATE
CONTRACT NO. AF 19(604)-2071
LAURENCE G. HANSCOM FIELD
BEDFORD, MASS.

administered by:

THE UNIVERSITY OF MICHIGAN RESEARCH INSTITUTE ANN ARBOR

August 1960

ACKNOWLEDGMENTS

Acknowledgments are due to Dr. K. T. Hecht for his innumerable suggestions and criticisms, and to Dr. Robert Terhune for his interest and advice, as well as for his major part in the work on derivative absorption spectra.

TABLE OF CONTENTS

LIST OF FIGURES

LIST OF FIGURES (Concluded)

CONTENT AND SUMMARY

overtone of each. Values of the polarizability components were determined from the intensities of the lines.

V. STARK EFFECT OBSERVATIONS

Stark effect observations in the vibration spectra of several simple polar molecules are reported. The most extensive work was done on HCN, and the dipole moment of the molecule in the excited vibration state ν_1 was evaluated. Stark difference signals were found in the case of CH_3F and CH_3I to be a valuable aid in the identification of the rotational fine structure of the vibration bands. In the case of NH_3, it is shown that the mixing of the wave functions due to the perturbation of the electric field permits transitions from which the inversion splitting in the ground and excited vibrational states may be calculated. The Stark effect observations of H_2O show that the largest effects arise from near-degenerate interacting levels.

I. INTERFEROMETRY

The advantageous position of an interferometer relative to a diffraction grating with respect to luminosity and potential spectral resolution has been pointed out by Jacquinot[1] and others. Some of the problems involved in its use might well be cited also, as for example the necessary separation of overlapping orders of interference (either optically or by the analysis of the spectral scan into frequency components), the limited free spectral range, and the spectral scanning mechanism—all of which are interrelated. Our choice of an interferometer system was seemingly the simplest one—a Fabry Perot, with overlapping orders removed optically, and a detector sensing the central fringe or axial intensity as the optical separation of the parallel reflecting surfaces changed. The reflecting surfaces were multilayer films of zinc sulfide and cryolite deposited on 2-1/2-in.-diameter fused quartz discs that were flat to 0.01 fringe of sodium light. The film stacks had a high reflectance (calculated at 99-1/4% for the 3-μ region) and the plates a commensurate flatness in order to gain a large free spectral range by operating at a low order of interference with a small separation of the plates. The variations in the thickness of the multilayer films and/or distortions of the flats caused by their mounting led to an over-all flatness of 0.1 fringe. The resulting mismatch between the high reflectivity of the films and the quality of the surfaces drastically reduced the luminosity and/or the resolving power of the system.

The interferometer plates were mounted on parallelogram-type tables of Invar similar to the design used by Kline.[2] The separation of the plates could be varied manually by a spring drive, or electrically by means of two U-shaped solenoids facing each other beneath the plates. The plates maintained their parallelism within 0.1 fringe over a 24-hour period. Overlapping orders were rejected by a grating monochromator operated at a 2-cm^{-1} band pass. The interferometer was placed in series with the monochromator, with KBr lenses for the collimator and telescope. The plate separation was about 1 mm.

Figure 1 shows a trace of the absorption of NH_3 observed by scanning with the solenoid drive of the interferometer. A resolution of about 0.3 cm^{-1} is indicated. A spectrum of the same region obtained with a high-resolution grating spectrometer operated at similar resolution is also shown in the figure. The interferometer's performance does not appear impressive, but it was operated at "slit widths" sufficient to give a resolution of 0.02 cm^{-1}. The signal-to-noise ratio under these conditions is encouraging, but the decreased resolution serves notice of the care that must be exercised with the plates. Although the low resolution of this trace furnished no real test of the solenoid drive, other experiences showed it to be inadequate for a fine scan.

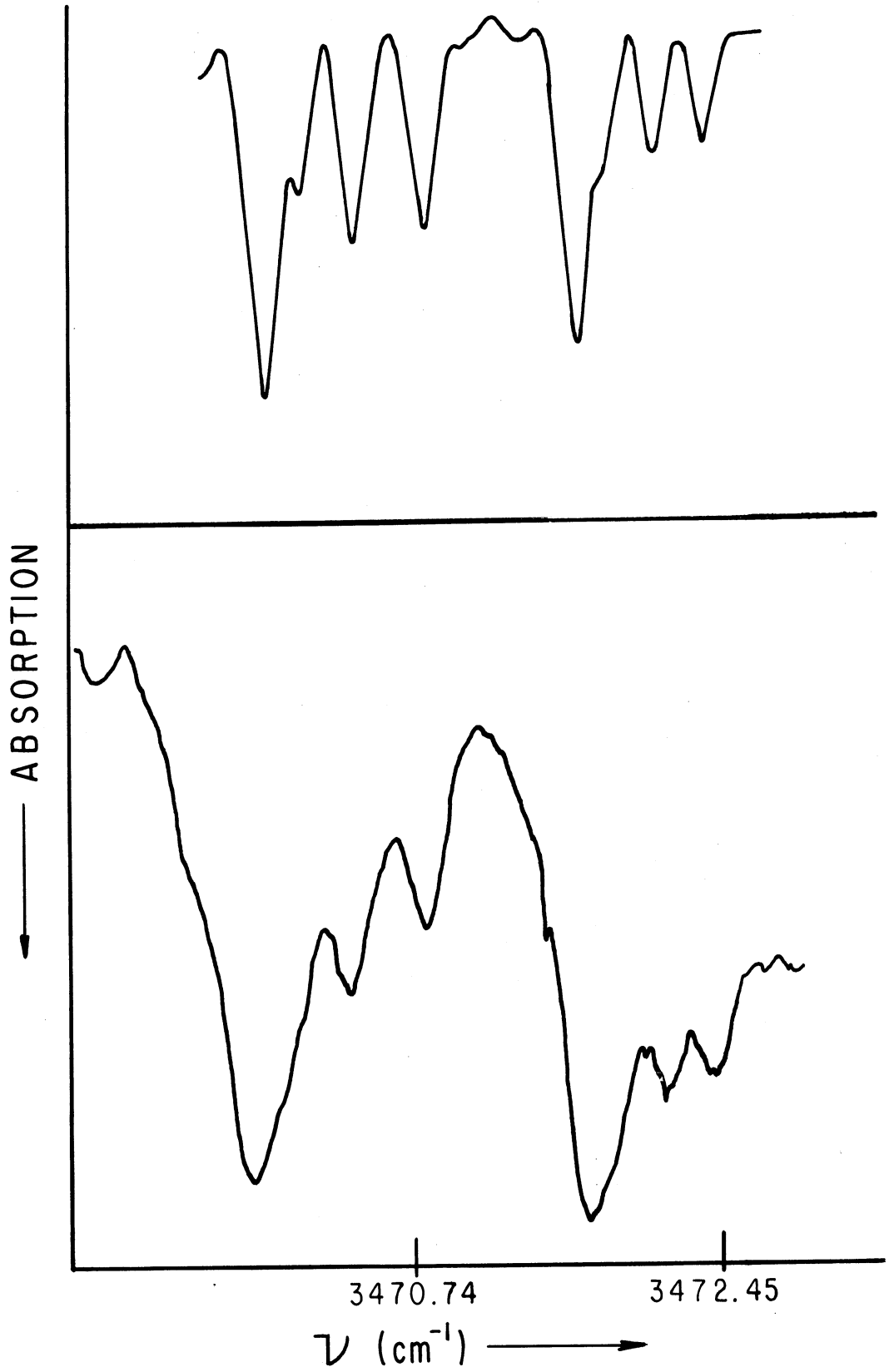

Fig. 1. R(6) of ν_1 of NH_3. Lower trace: Spectrum obtained with Fabry-Perot inferometer in series with low-resolution grating spectrometer. Upper trace: Spectrum obtained with high-resolution grating spectrometer.

Designs were made for a tandem Fabry-Perot system with etalons scanned by air pressure variation, coupled with a low-resolution grating monochromator to achieve a resolution of 0.003 cm^{-1} in the 3-μ region. However, the backlog of work in the instrument shop promised such a delivery date that it was deemed sensible to suspend plans for it in favor of other projects less demanding of machine work—in particular, electric field effect measurements.

These Stark effect observations have in turn rekindled interest in a high-resolution interferometer. The reduced line width would yield more profuse and more accurate data since the limited frequency interval between adjacent rotational lines sets the limit on both the detection and interpretation of the Stark shifts (the latter because the shifts of the levels become highly complicated when the Stark splitting approaches the separation of the rotational lines). The major change in the plans for the system has been to couple a grating monochromator of moderate resolution (0.25 cm^{-1}) to a single Fabry Perot by means of infrared transmitting fibers imaging the slit of the grating spectrometer onto the circular aperture of the interferometer.

II. DERIVATIVE ABSORPTION SPECTRA

INTRODUCTION

The derivative of the spectral transmission curve of a sample may be obtained in a variety of ways. The simplest, though most tedious, is by graphical measurement of the slope of the recorded transmission curve. This operation can be done automatically by the electronic analysis of the output of the detector as has been reported by Martin.[3] However, methods which result in an output signal from the detector of the monochromator that is proportional to the derivative of the transmission curve possess a number of advantages relative to both the derivative curve obtained as above and also to the usual transmission curve itself. First, the location of maxima and minima, the usual points of interest in a spectrum, is accomplished by a null measurement. Further, since the constant signal falling on the detector is ignored and only differences between two closely adjacent wavelengths are amplified, the noise observed is that characteristic of the frequency at which the adjacent wavelengths are alternated on the detector, and other frequency components of noise and drift are rejected by the amplifier. In addition, in the case of weak absorption lines, effectively only deviations from the envelope of the spectral energy transmission curve of the instrument are recorded, and the scale of the recording can be varied by changes of the amplifier gain without the necessity of biasing voltages to stay within the limited range of the recorder.

The oscillation of any optical component of the spectrometer that will cause two adjacent wavelengths alternately to fall upon the detector will generate in the output of the detector a signal of the same frequency whose magnitude is proportional to the first derivative of the transmission curve being scanned. Giacomo and Jacquinot[4] have used in this way a vibrating mirror placed in the beam beyond a wide exit slit to locate the transmission maxima of evaporated thin films. (A subsequent narrower slit determined the spectral band pass, and the spectrum was oscillated relative to this second slit.) French and Church[5] have incorporated a vibrating exit slit into a monochromator to produce a first derivative output in the study of overlapping absorption bands. Pemsler[6] has achieved the same result in the case of a Perkin Elmer Model 21 Double Beam Spectrophotometer by a deliberate misalignment producing a fixed wavelength displacement between the two beams.

PROCEDURE

As has been mentioned, there is complete freedom in the choice of the optical element that is to be periodically displaced so as to oscillate the spectrum across the exit slit, and it does not matter whether it lies in the collimated or uncollimated portion of the optical path. The displacement of the

beam is so slight in all cases that no problems of vignetting arise. For example, the prism or grating of the spectrometer could be vibrated, or the plane mirror of a Littrow system. In practice, however, it is simplest to drive as small a mass as possible. Therefore the moving element should be near a focus—either the entrance or exit slit—where the beam has a reduced cross-sectional area, and the optical element may be correspondingly small. Likewise, since it is located near a focus, its optical quality need not be as high as otherwise.

A thin wedge prism of a transparent material may be inserted into the beam either after the entrance slit or before the exit slit so as to produce the desired effect when the wedge is moved. This arrangement has the advantage that the path of the rays through the spectrometer is unchanged except for a slight shift in focus, and the mode of operation could be quickly changed by adding or removing the prism. The wedge of prism angle A produced a small displacement of the spectrum at the exit slit, x, given by:

$$x = (n-1)\, A\, y$$

where n is the refractive index of the wedge, and y is the distance from the slit to the wedge. The magnitude of x desired is of the order of the width of the slit, and small values of A and y will generally be sufficient. In addition, the amplitude of the motion can be varied by altering y. The spectrum can then be displaced periodically in several ways, as (1) by lateral insertion of the wedge into and out of the beam, (2) by an oscillating motion of the wedge longitudinally along the beam, or (3) by a rotation of the wedge at constant speed about an axis parallel to that of the beam. In the last case, there is also a periodic vertical displacement; but because the slit is usually considerably longer than wide, the resultant modulation is small, and if the detector "sees" slightly more than the normally illuminated length of slit, the effect will be negligible.

The desired motion of the spectrum can also be produced by an oscillating mirror placed near a slit so as to deflect the beam. This arrangement was convenient for the particular instrument with which the work was done—a 1-meter focal length, f/5, Pfund-type grating spectrometer described by Hardy.[7] In this case, a 1-cm-square mirror cut from a microscope slide was placed about 5 cm before the exit slit and deflected the beam at 90° onto a new exit slit formed by razor blades. This mirror was mounted as a torsion pendulum, being glued to a thin iron sheet which in turn was glued to the middle of a 3-cm-long, thin steel wire fastened at its ends. A small hand-wound electromagnet was mounted just behind one edge of the mirror and gave approximately 1° rotation of the mirror per watt of power. The magnet was biased by a d-c current to prevent frequency doubling in the motion of the mirror when an alternating voltage was applied to the magnet. An angular rotation of the mirror of the order of 10 minutes of arc was sufficient to interchange adjacent spectral band passes of the instrument.

Measurements were confined to the 2- or 3-μ region. A 500-watt projection lamp was used for a source. The grating was a 7200-line-per-inch replica, and its higher orders were removed by a germanium filter. An uncooled Eastman Kodak Ektron PbS cell, 2.5 x 0.25 mm, detected the radiation. This cell itself served as the new exit slit. A sizable gain in signal strength could have been obtained by placing it at the focus of a condensing ellipsoidal mirror to collect flux from a longer slit. The chopping or oscillation frequency of the mirror, as well as the frequency in the output of the detector that was amplified electronically, was 90 cps.

Normal absorption spectra were obtained with the small mirror stationary and a 90-cycle chopper interrupting the radiation. The signal, after passing through a tuned 90-cycle amplifier, was recorded after either rectification in the normal manner or else by a lock in detection system using a synchronizing signal from the chopper. To observe the derivative spectra, the chopper was removed from the beam, and the mirror was driven at 90 cycles by applying an amplified portion of the synchronizing signal from the chopper to the magnet. Exactly the same amplifying system was used as above.

The appearance of the several types of spectra is shown in Fig. 2. Fig. 2a represents the normal trace of an absorption line. With an oscillating optical element, the detector alternately sees curves A and B of Fig. 2b as the grating is turned, and the a-c output of the detector is proportional to the difference between the two curves. After normal rectification of the amplified a-c signal, the trace of Fig. 2c results, whereas synchronous rectification preserves the phase of the signal, so that positive and negative excursions from zero are recorded as in Fig. 2d.

The derivative spectrum of atmospheric transmission in the wing of the 3750-cm^{-1} water vapor fundamental with an air path of about 6 meters is shown in the lower trace in Fig. 3, using normal rectification, along with the normal spectrum. The zero of the normal spectrum on this and subsequent figures is the base line of the figure. The peak of an absorption line, or more properly the point of zero slope, is clearly indicated by the sharp central dip in the derivative. This has been utilized in other spectral regions to enhance the accuracy of line measurements. Any asymmetry in the shape of an absorption line is revealed by an inequality in the two lobes of the derivative. The slope of the envelope of the spectral energy curve is not large enough to be apparent in the differentiated spectrum at this gain, and only excursions from the envelope appear. This permits a convenient method of expanded scale recording in which only the signal of interest, i.e., a change in the transmission, appears. If the signal-to-noise level is large, information on small changes in transmission that would otherwise be lost is clearly displayed. For example, the indicated weak water vapor line, absorbing about 1-1/2% of the incident energy in the normal spectrum, is sizably magnified in the differentiated spectrum, on which no noise is apparent. Variations in the amplitude of oscillation of the mirror changed the magnitude of the derivative trace, but

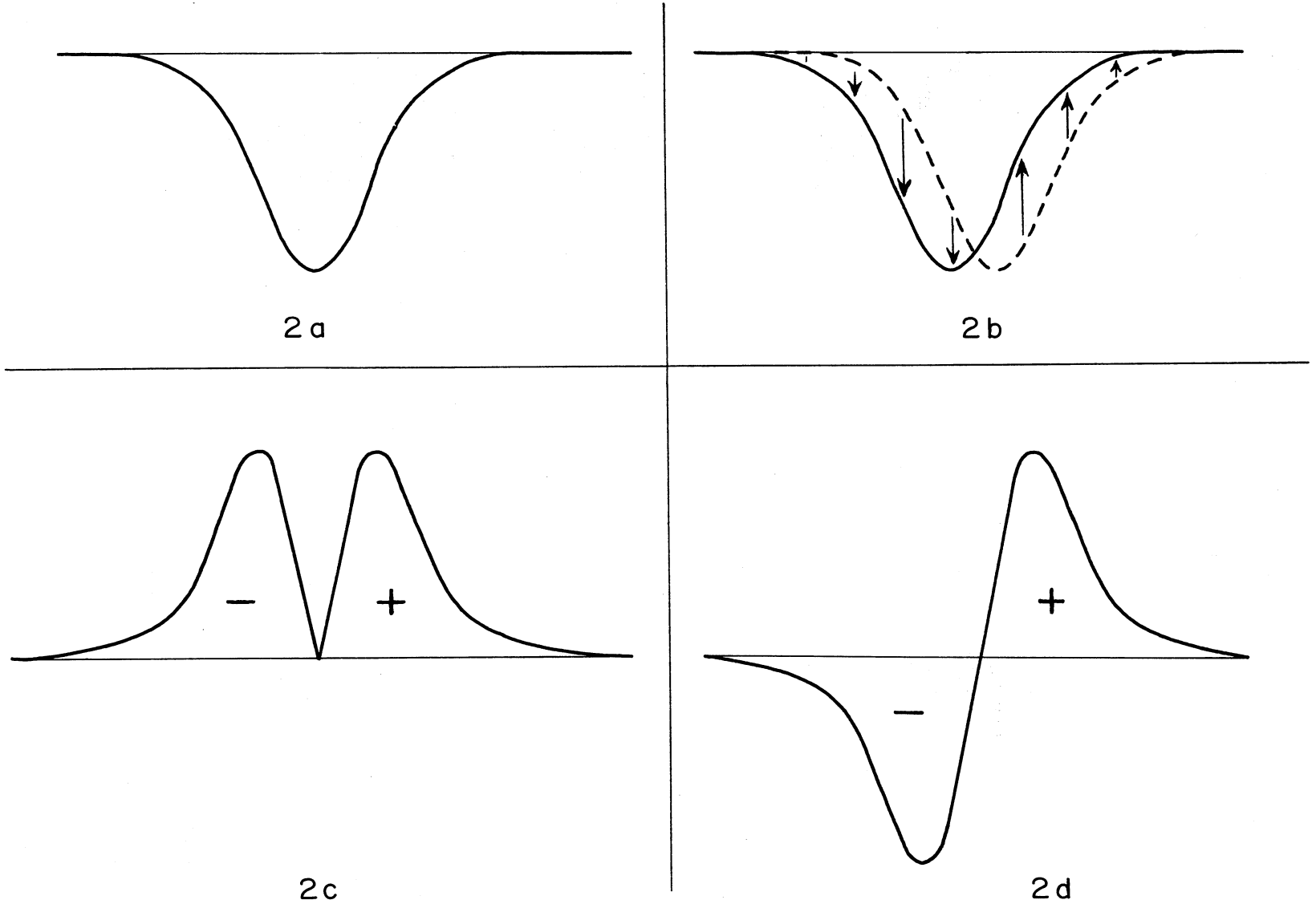

Fig. 2. Signal vs. angular position of grating. (a) Normal spectrum of an absorption line. (b) Individual signals on alternate phases of oscillation of the mirror--the arrows indicating the difference signal. (c) Difference signal with normal rectification. (d) Difference signal with phase-sensitive rectification.

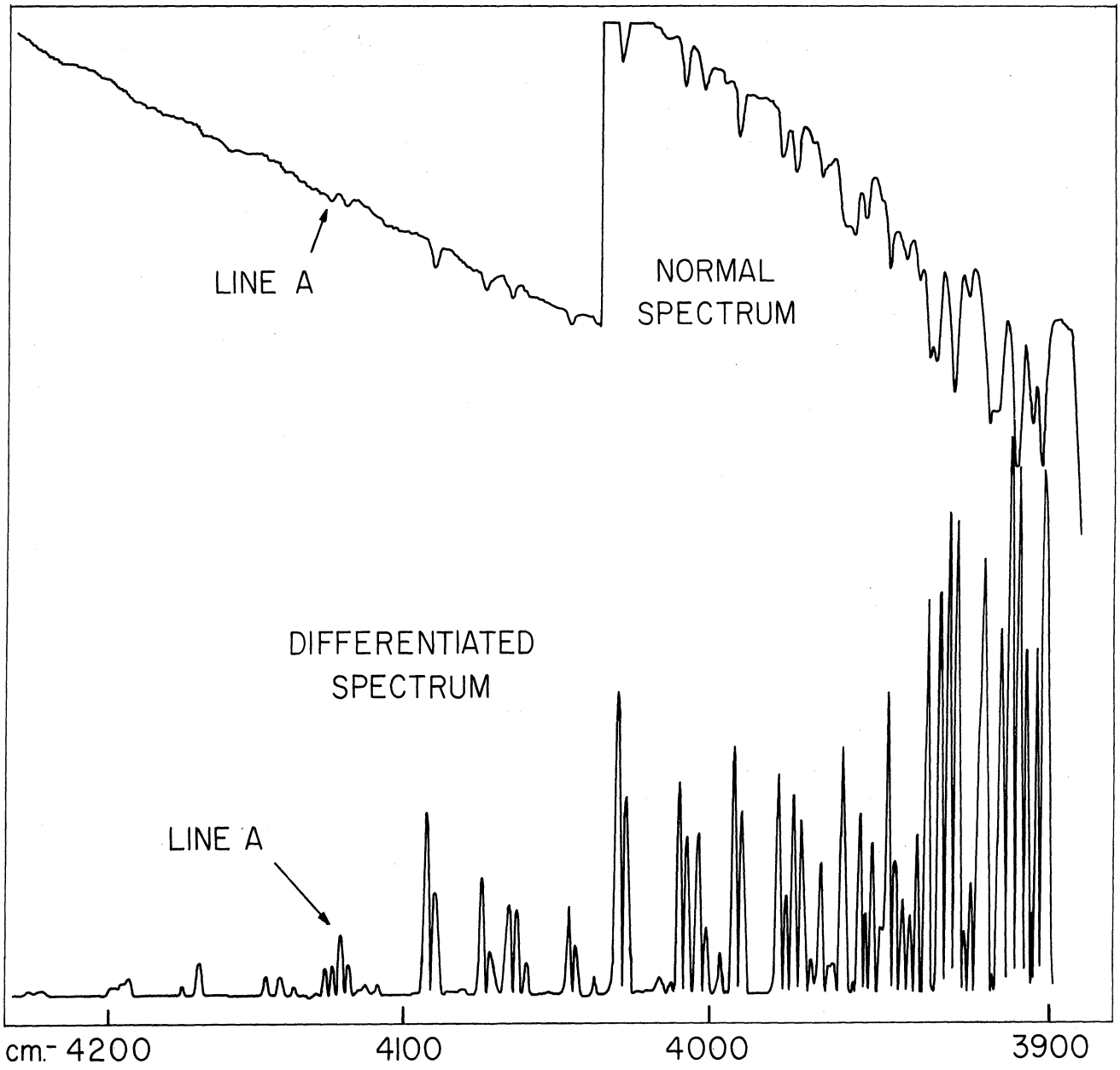

Fig. 3. Atmospheric transmission, 3900- to 4200-cm^{-1} region, 6-meter path, 2-cm^{-1} spectral slit width. Change of scale x 3/2 at 4035 cm^{-1} in regular spectrum. Normal rectification in the first derivative spectrum.

had little influence on its appearance until quite large amplitudes were reached, when the resolution suffered.

The gain can be greatly increased before any noise becomes visible, as shown in Fig. 4. This and all subsequent records were made with the lock in detection method. The scale can be realized by reference to the same 1-1/2% absorbing water line. The regular structure on the high-frequency side is not characteristic of water vapor, and was traced to interference effects in the Multilayer germanium filter and also the glass substrate of the PbS detector. A smear of grease on the back surface of the detector eliminated the latter and a much thicker germanium filter (1/8 in.) did not show any interference effects at this spectral resolution.

After these changes, the derivative trace of atmospheric transmission between the 3750- and 5330-cm^{-1} water vapor bands was recorded at high gain as shown in Fig. 5. The appreciable slope of the envelope of the spectral energy curve of the apparatus causes the over-all drift of the differentiated curve at this amplification. The signal level has changed by more than an order of magnitude in the spectral interval, however.

The first overtone band of CO at 4260 cm^{-1} was used to demonstrate the detection of small changes in transmission in regions of large signal-to-noise ratio by means of the derivative technique. The upper curve of Fig. 6 shows the absorption of 1 atmosphere of CO in a 10-cm cell with 2-cm^{-1} resolution; and the lower curve, the differentiated spectrum under the same conditions. Reduction of the CO pressure to 2 cm of Hg removed nearly all trace of absorption in the normal spectrum as in the upper curve of Fig. 7. The lower curve of Fig. 7 is the derivative spectrum recorded at high gain, and the inherent details of the spectral transmission are revealed. The signal-to-noise ratio, in this case, was 5000 to 1 at a response time of 1 sec and a spectral slit width of 2 cm^{-1}. Assuming a linear relation between absorption and pressure, the least perceptible change in the derivative curve corresponds to a change of transmission of 1 part in 4000. Significantly greater sensitivity could be obtained with a more perfect grating and by using a cooled detector with an ellipsoidal mirror to demagnify the image of the slit. With these improvements, S/N values of 100,000/1 have been realized at 1-sec response time and 1-cm^{-1} resolution. This ratio may be further increased by the use of longer response times to reduce the noise, or by wider slits at the expense of resolution to increase the signal until saturation of the detector occurs. (At 4000 cm^{-1}, the saturation limit of an uncooled PbS cell appeared to be near 10^5/1 at a 1-sec response.)

One might expect that the normal spectrum observed at high gain with the recorder zero offset by a biasing voltage would show the same detail. Such a trace of the background near 4200 cm^{-1} is given in Fig. 8, with the gain increased by a factor of five. A section of the curve shows the noise with the spectrometer scan stopped. By comparison with the derivative curves of Figs.

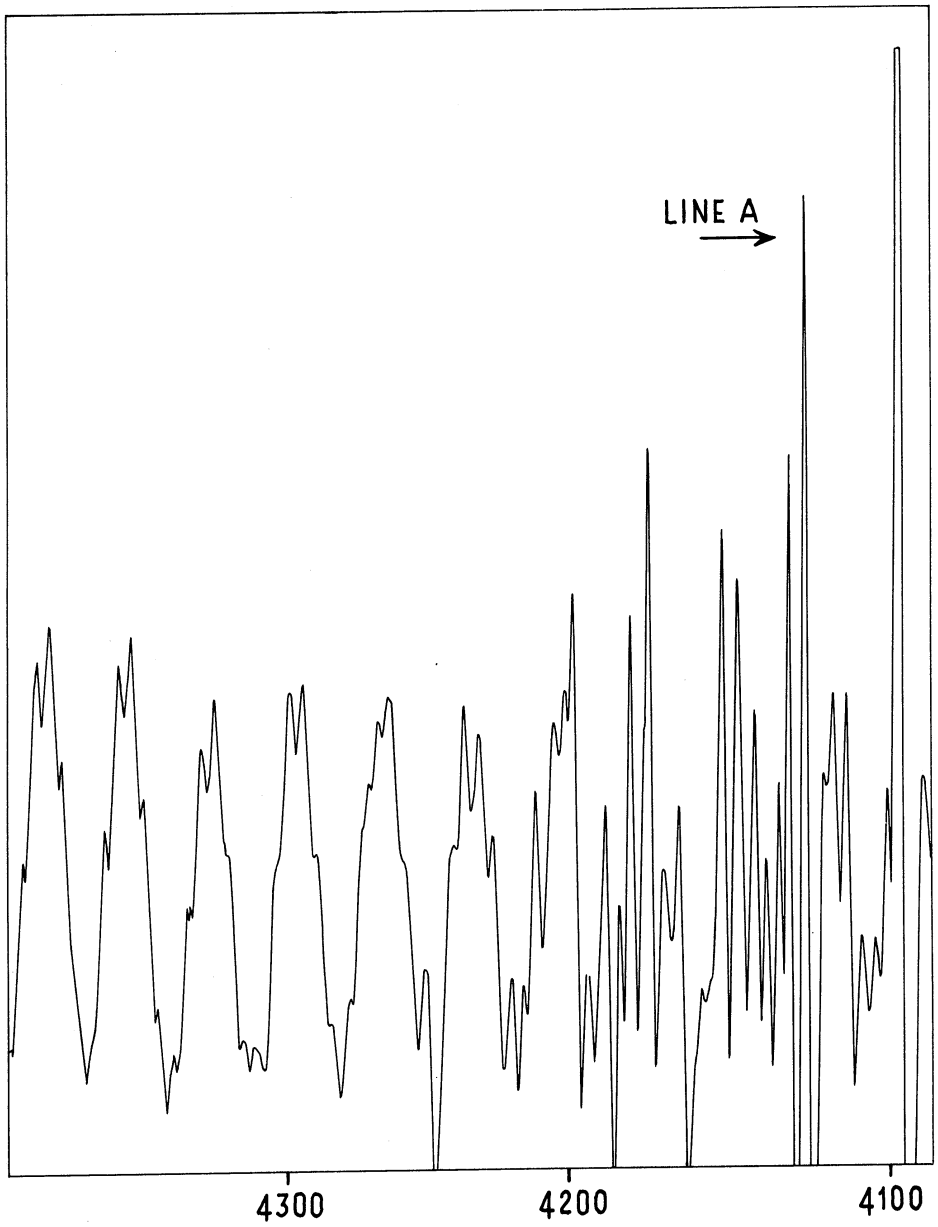

Fig. 4. First derivative of atmospheric transmission curve as in Fig. 3 but with synchronous rectification and higher amplifier gain.

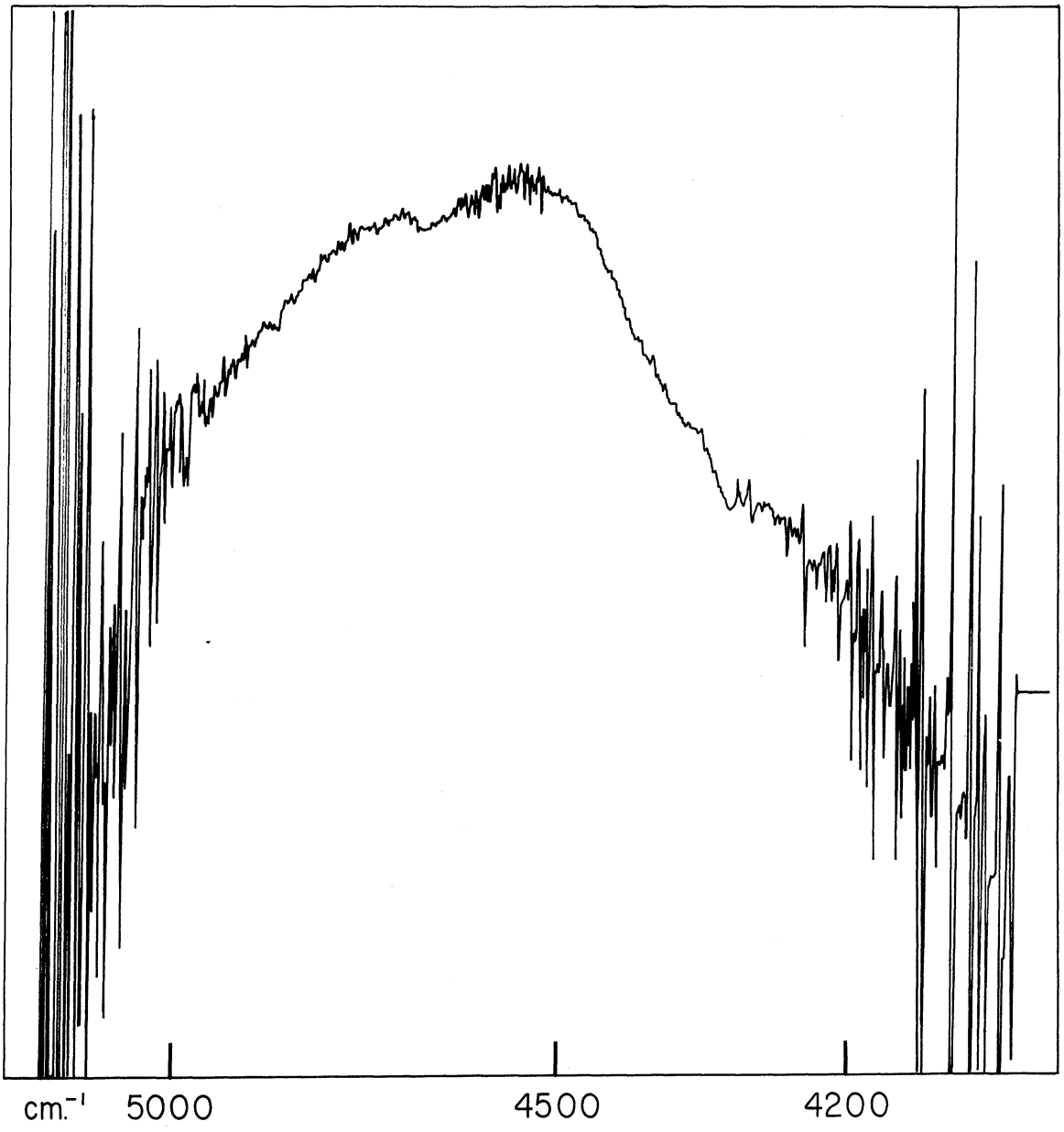

Fig. 5. First derivative spectrum of atmospheric transmission, 4000-5000 cm^{-1}, 6-meter path, 2-cm^{-1} spectral slit width, synchronous rectification, high gain.

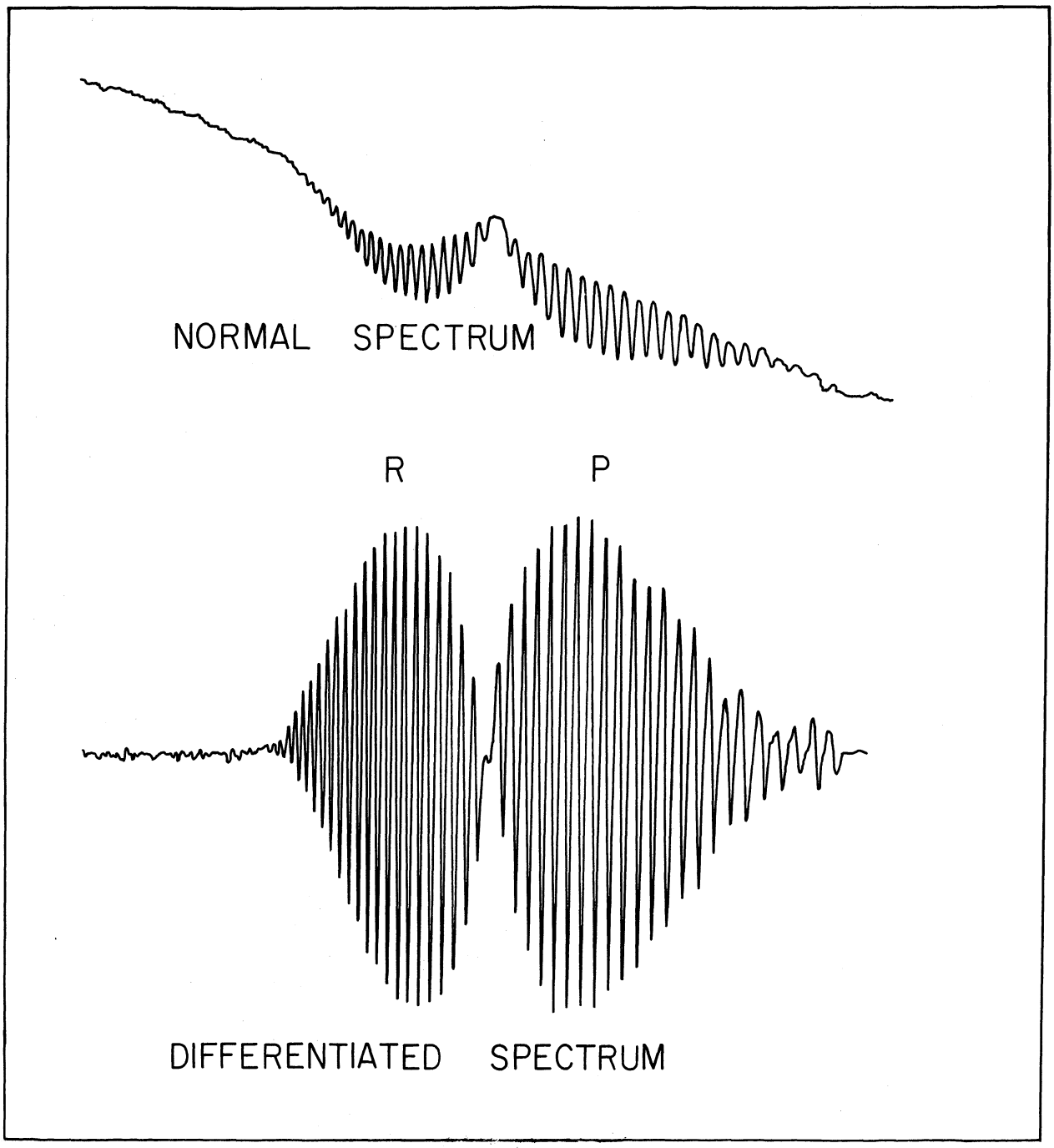

PRESSURE: 1 atm. PATH: 10 cm.

SLIT: 2 $cm.^{-1}$

Fig. 6. Normal and first derivative spectra of CO overtone absorption at 4260 cm^{-1}, 1 atmos. CO, 2-cm^{-1} spectral slit width.

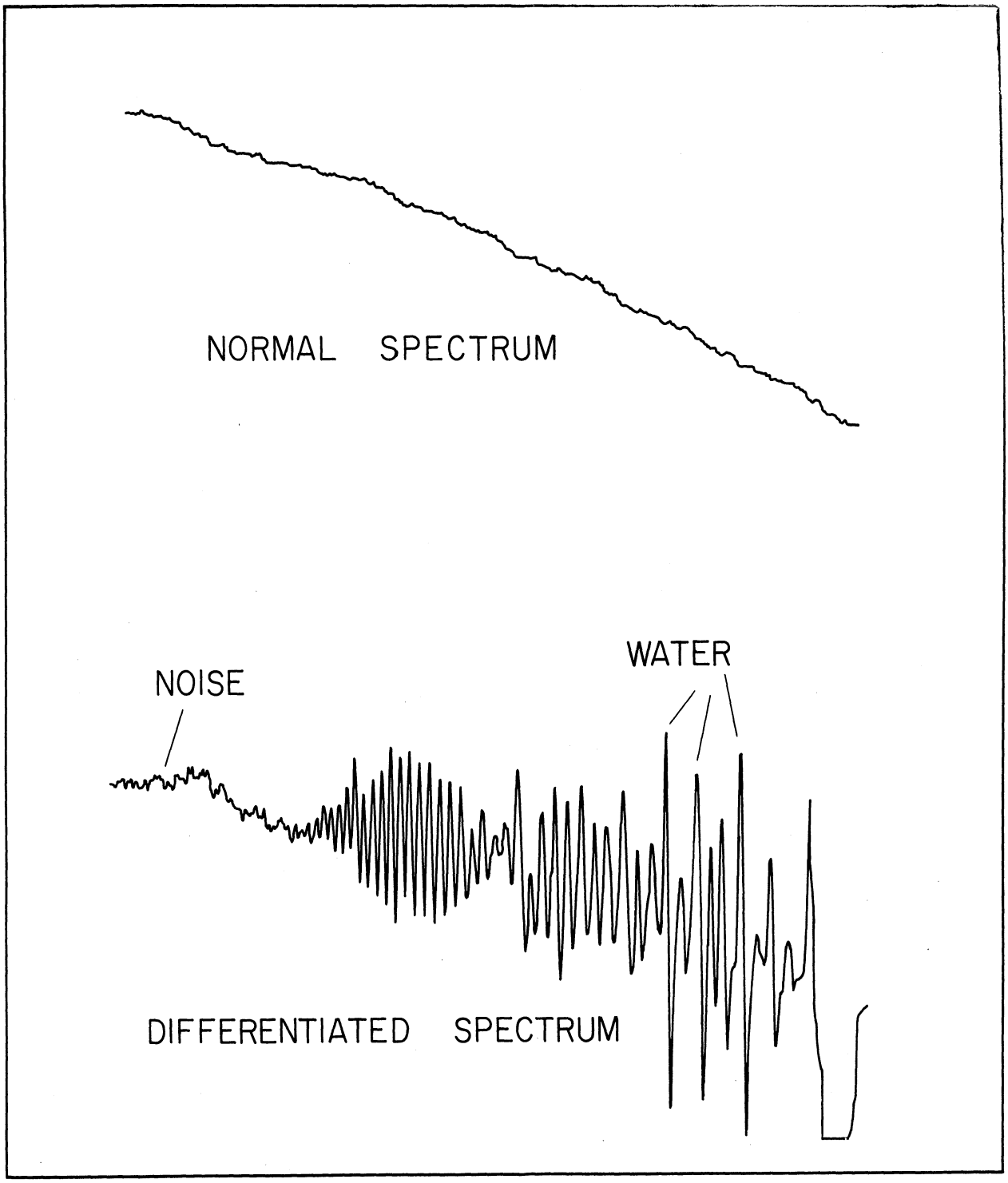

Fig. 7. Normal and first derivative spectra of 4260-cm^{-1} CO band at reduced concentration. Pressure, 0.03 atmos., 10-cm path, 2-cm^{-1} spectral slit width.

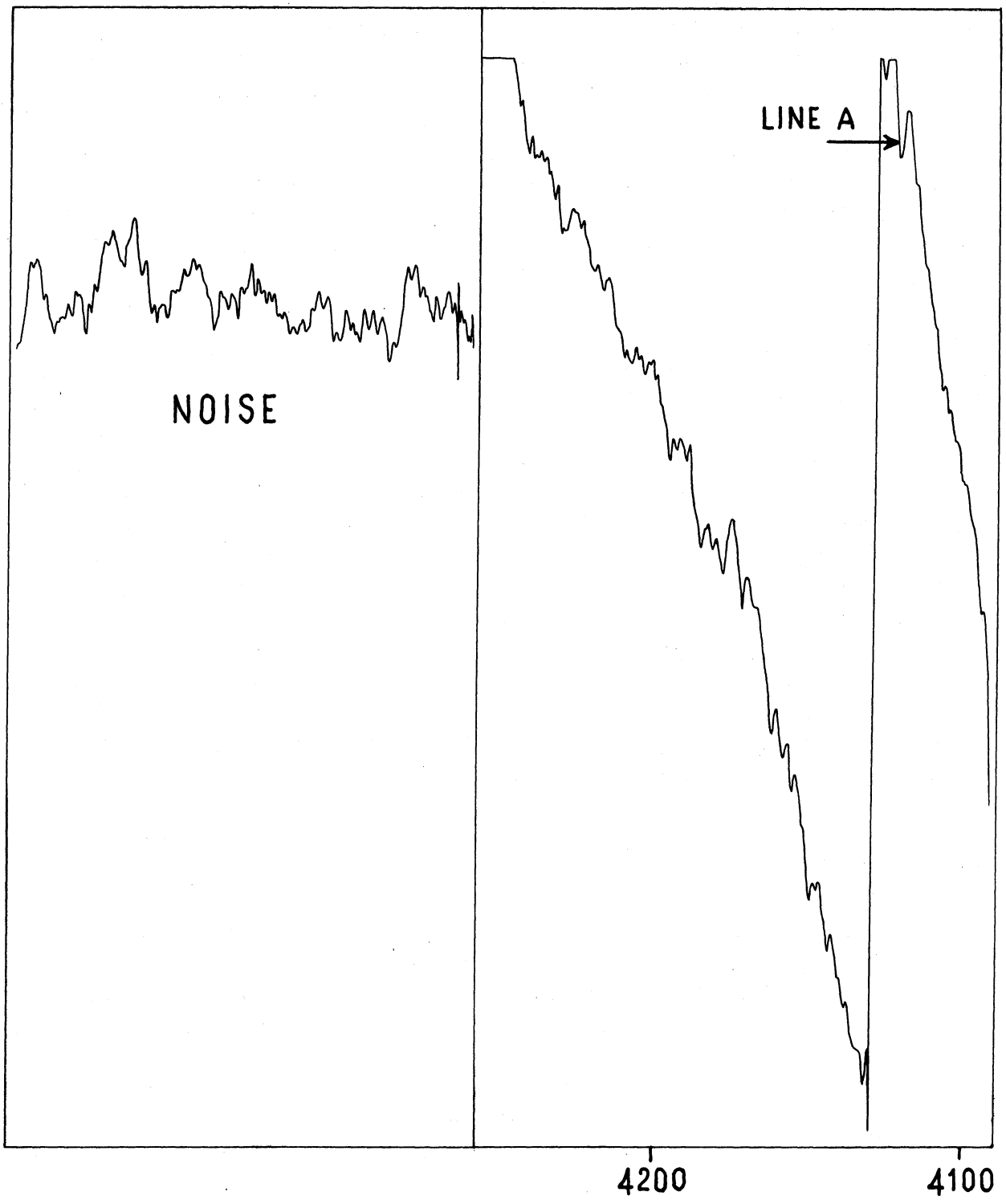

Fig. 8. At right: Normal spectrum of atmospheric transmission, 4100-4200 cm^{-1}, as in Fig. 3, except higher amplifier gain (X 5) with bias voltage adjusted to keep recorder on scale. At left: Noise trace with grating drive stopped.

3, 4, and 5, two disadvantages are apparent: the steep slope of the envelope (increased by the same factor as the gain) that demands frequent readjustment of the biasing voltage; and that the noise level is an order of magnitude larger than for the derivative spectra. The higher noise level is a consequence of the noise spectrum of the source and most other disturbances such as air currents, vibrations, etc. All these have noise that is predominantly of low frequency. In the case of the source, for example, the large thermal mass prohibits rapid changes. In a normal spectrum obtained with an on-off chopper, the absolute size of the signal from the radiant flux of the source is being examined at 90 cycles, and slow changes in the size of this signal will be registered. With the derivative technique, as in a difference system, only the change in the signal level from one half-period to the next (1/180 sec) is amplified. This advantage relative to noise level is not peculiar to the derivative system but holds for any double beam of difference spectrometer.

The accuracy of the trace obtained with the oscillating mirror in representing the first derivative of the spectrum was tested by integrating the trace and comparing the result. The normal spectrum and derivative trace are shown in Fig. 9 using a 10-cm path of CO at one atmosphere pressure and a spectral band pass of 3.5 cm^{-1}. The distortion of the R branch in the spectrum is due to a match of the line spacing with the rectangular band pass of the spectrometer. The derivative trace was integrated by an electro-mechanical gadget and the resultant curve is plotted in Fig. 10 on an arbitrary scale. By comparison with the normal spectrum, it appears that nothing has been lost or added in the process of differentiating and integrating, and one may conclude that the technique does produce a trace proportional to the first derivative of the spectrum.

SUMMARY AND CONCLUSIONS

Any one of several simple modifications can be made to a monochromator to produce an output signal from the detector that is directly proportional to the first derivative of the spectrum being scanned. A signal proportional to one of the higher derivatives could be obtained if desired by properly vibrating one of the optical elements of the monochromator. For example, a trace of the second derivative could be obtained from the component of the detector's output of frequency f if the spectrum were sinusoidally modulated across the exit slit at a frequency f/2, as has been pointed out by Giacomo and Jacquinot.[4]

The chief advantage of directly generating a signal from the detector that is directly proportional to the first derivative of the spectrum over the normal spectrum itself is that a difference measurement is made. In spectral regions where there exists a large signal-to-noise ratio, the noise level is not infrequently determined by factors associated with the source and optical path rather than the detector. In extreme situations of this sort, an order-of-magnitude improvement in the signal-to-noise ratio can be realized by the use of the derivative technique. A good example of this occurs in solar spectroscopy where the noise level is presumed to be set by atmospheric fluctuations.

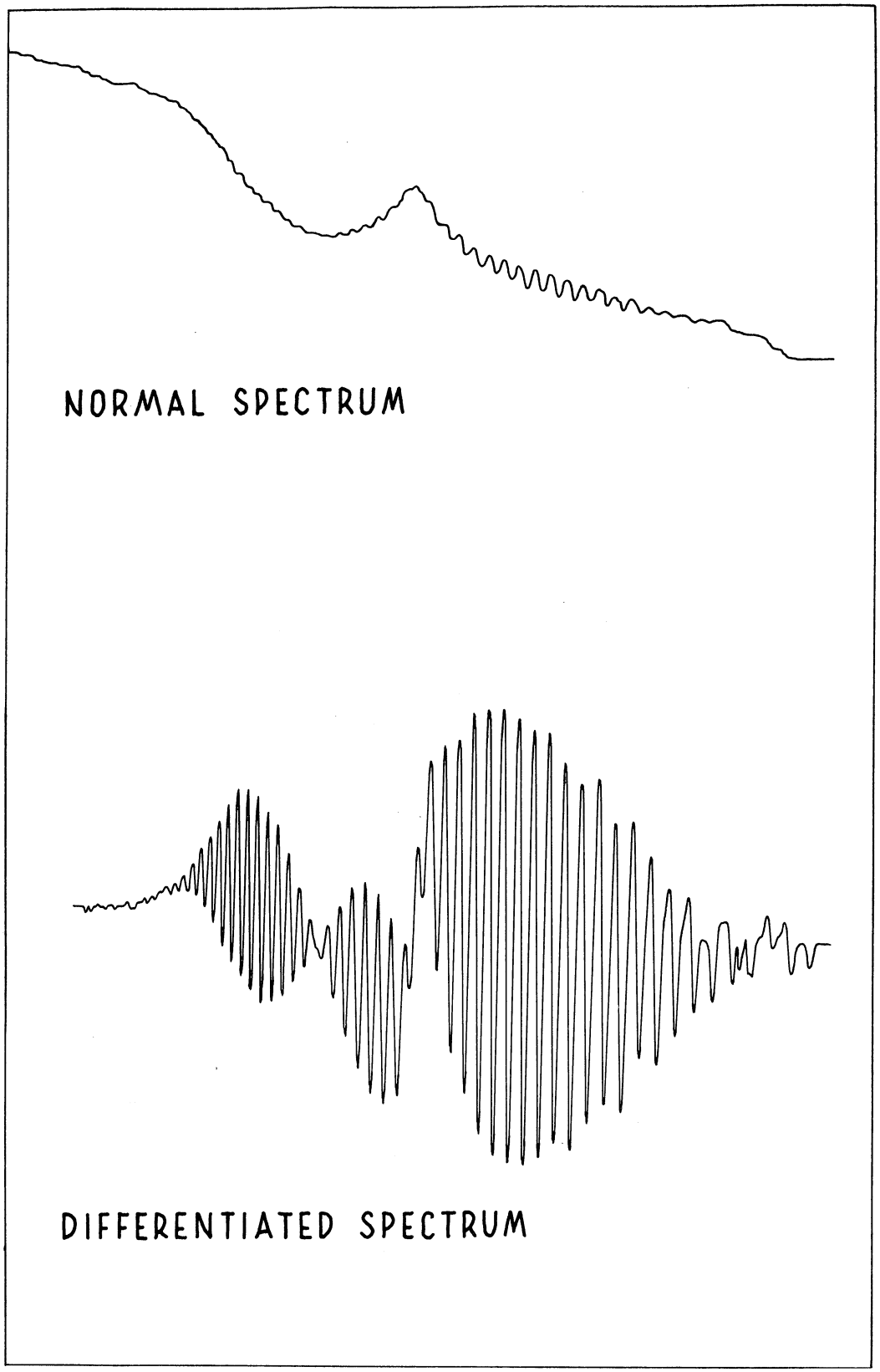

Fig. 9. Normal and first derivative spectra of 4260-cm^{-1} CO band, 1 atmos. pressure, 10-cm cell, 3-cm^{-1} spectral slit width.

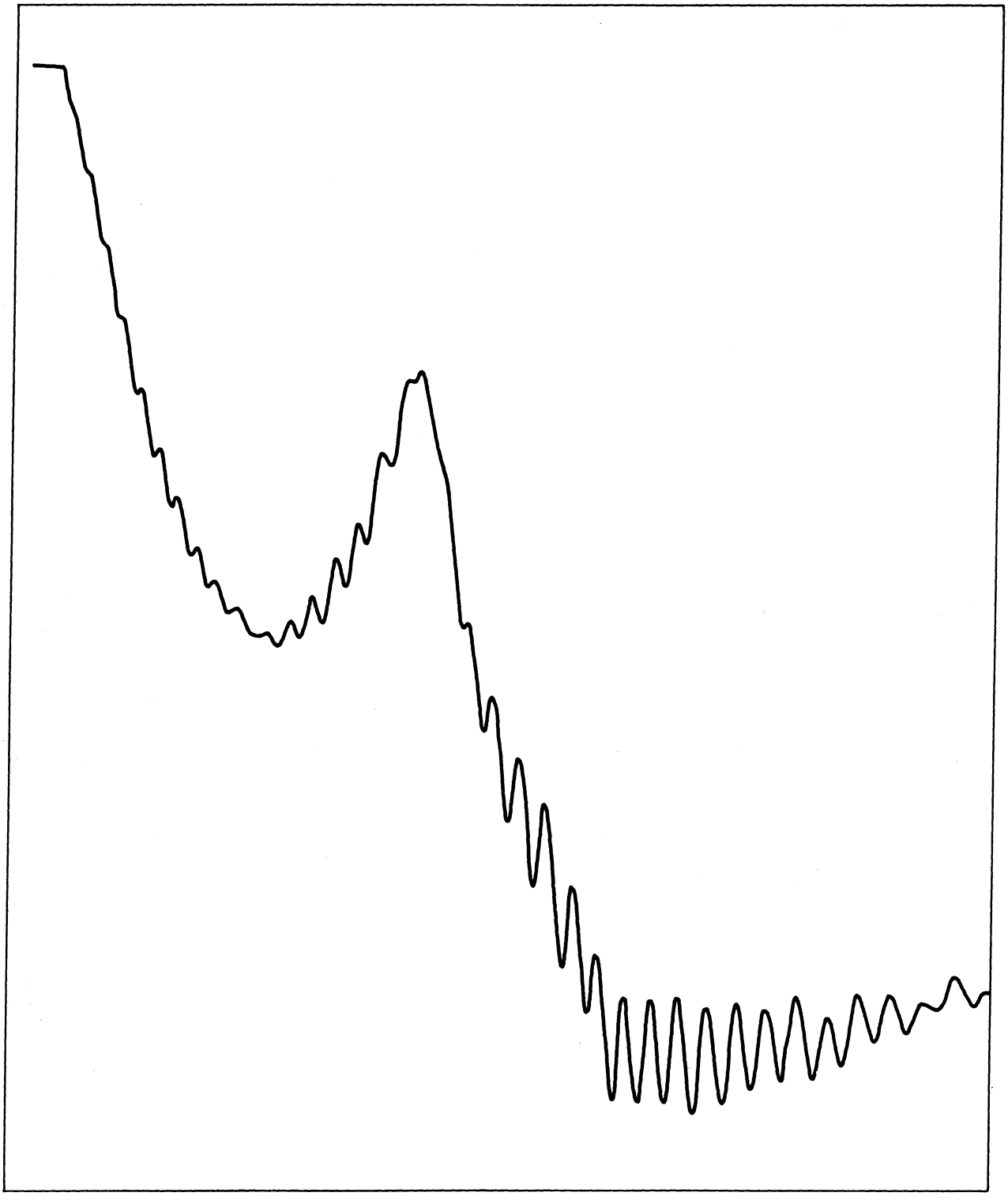

Fig. 10. Integrated trace of the first derivative spectrum of Fig. 9 on an arbitrary scale, to be compared with the normal spectrum of Fig. 9.

The use of the first derivative of the spectrum also provides an escape from the limited dynamic range of the recording system when one is interested in observing small percentage absorptions. In the derivative trace, the signal to the recorder is proportional to the absorption of the sample, not to the transmission through it as in the normal spectrum. Since excursions from zero are being measured, the scale of the recording can be altered by a change in the gain of the amplifier without going off scale except for large absorptions. A double-beam instrument operates similarly, but double-beam units are not available for all monochromators nor are they suitable for all problems (solar spectroscopy, for example). In operation in the derivative mode in conjunction with a high-dispersion instrument and a sensitive photoconductive detector, extremely small absorptions and consequently concentrations could be detected, as is indicated by the data on the overtone band of carbon monoxide.

III. FAR-INFRARED ABSORPTION SPECTRUM OF H_2O_2

Although H_2O_2 is the simplest molecule possessing a hindered internal rotation, relatively little work has been done on its rotational energy levels and the resulting spectral transitions. In large part this may be attributed to the experimental difficulties resulting from its chemical instability. Not only is the material very reactive at room temperature, but its vapor pressure is relatively small so that the sample must be heated to obtain sufficient absorption, thereby increasing the rate of decomposition. Finally, its decomposition product H_2O has both strong vibration and rotation absorption spectra that overlap the spectral regions in which H_2O_2 is absorbing.

Giguère[8] has examined the vibration spectrum and made an assignment of the fundamental vibrations on the basis of a nonplanar model having C_2 symmetry. In several bands he noted a doubling of the lines which he attributed to the effect of the internal rotation of one OH group relative to the other. Massey and Bianco[9] examined the microwave spectrum and found nine lines in the 9000-40,000 Mc/sec region. They were able to obtain qualitative agreement with their data by approximating the hindering potential with a sine function. Massey and Hart[10] considered the case of an asymmetric hindering potential (high at the cis position and low at the trans position of the OH groups when planar). They showed that each rotational level is then split into a symmetric and antisymmetric state (much as in the case of the inversion doubling of NH_3), with a splitting of the order of $10 cm^{-1}$. However, it was not possible to uniquely to determine the heights of the cis and trans barriers.

The far-infrared spectrum should furnish enough additional information to solve the problem. As Massey *et al.* pointed out, H_2O_2 may be considered as a nearly symmetric top, its dipole moment perpendicular to the figure axis. The selection rules that apply to the pure rotation spectrum are $\Delta J = 0, \pm 1$, $\Delta K = \pm 1$, $a \leftrightarrow s$, $a \nleftrightarrow a$, and $s \nleftrightarrow s$. The strongest absorption should be associated with $\Delta J = 0$ $\Delta K = +1$—what might be called Q lines of a perpendicular band of a symmetric top. Given the values $B \approx .83 cm^{-1}$ and $A \approx 9.96 cm^{-1}$, these transitions would be expected to fall in the 10- to 150-cm^{-1} range. The $\Delta J = \pm 1$ $\Delta K = 1$ transitions would be individually weak and closely spaced, and behave somewhat like a continuous background absorption.

The far-infrared vacuum grating spectrometer designed by Randall and Firestone[11] has been modified for this work to have the source, detector, and absorption cell outside of the main vacuum chamber. An H-4 mercury arc was used below 100 cm^{-1}, and a heated platinum strip coated with carborundum dust above 100 cm^{-1}—either being imaged on the entrace slit with fivefold magnification by an off-axis ellipse. A glass blade chopped the radiation at 10 cps. Three scattering gratings attenuated the higher orders of interference of the grating, and the impurity appeared to be less than 5% throughout the spectrum. A 3-

traversal absorption cell of the Pfund type (2 perforated spheres separated by their focal length of 30 cm) was mounted after the exit slit. The cell was made of a Pyrex cylinder and Pyrex mirrors (which served as the end plates) with thin films of polyethylene glued over the holes in the spherical mirrors for windows. This cell was wrapped in a heating jacket and enclosed in a larger brass cylinder that served to take practically all the strain due to evacuation. The radiation was detected by a Golay cell with a polished tapered cone attached to it to demagnify the image. Through the use of long integration times, (a minute or more), records could be generally obtained with a resolution of 0.3 cm^{-1}. The H_2O_2 had to be heated to 60-70°C to obtain sufficient absorption in the 90-cm path, and the cell was pumped on slowly but continuously to remove the decomposition products while H_2O_2 evaporated into the cell to maintain the pressure. The 99% purity H_2O_2 was obtained from the Buffalo Electro-Chemical Company.

The stronger absorption lines are listed in Table I. These are preliminary values obtained by interpolation between water lines, with an estimated accuracy of 0.1 cm^{-1}. These were obtained by subtracting out the absorption of H_2O taken as a background spectrum with enough water vapor to give more or less similar line strengths for the H_2O lines. The concentration of H_2O_2 in the cell varied during any one run, as well as from run to run so that the relative intensities of the lines are not known. In addition, there are a number of weak lines in the spectrum possibly due to an accidental piling up of $\Delta J = \pm 1$ transitions. Massey and Hart[10] give the energy levels through $K = 4$, and the $\Delta J = 0$, $\Delta K = 1$, $s \leftrightarrow a$ transition frequencies in this range are also listed with the J, K, and symmetry identification. It is apparent that there are appreciable deviations from the predicted line positions already at $K = 4$. Further work is in progress to extend the observations down to the 15-cm^{-1} region.

The large number of lines occurring in the 140- to 200-cm^{-1} region probably involve transitions to the first excited state of the torsional motion. In addition, Prof. Hecht has set up the hindering potential problem for calculation by an IBM 704 computer, and it is hoped that specific values for the barrier heights as well as their dependence on K may be found. An exploratory run of the spectrum in the 3400-cm^{-1} region has been made at much higher resolution (0.05 cm^{-1}) but no real effort has been made to understand its complex structure as yet.

TABLE I

ABSORPTION FREQUENCIES OF H_2O_2 IN THE FAR-INFRARED

Observed Strong Infrared Absorption Lines	Transitions Predicted by Massey and Hart[10] (up to K = 4)	
52.25 cm^{-1}	15.7 cm^{-1}	2,1,a → 2,2,s
53.2	19.3	1,0,a → 1,1,a
70.8	31	3,2,a → 3,3,s
71.3	37.7	2,1,s → 2,2,a
89.7	50	4,3,a → 4,4,s
94.0	55	3,2,s → 3,3,a
109.28	74	4,3,s → 4,4,a
112.53		
130.51		
135.52		
142.2		
143.3		
144.0		
148.7		
153.2		
154.2		
155.9		
160.9		
162.0		
162.7		
184.9		
188.3		
192.8		
196.1		
197.7		
215.4		

IV. ABSORPTION OF H_2 AND D_2 INDUCED BY AN ELECTRIC FIELD

The electric field induced absorption of the normally infrared inactive vibration-rotation bands of H_2 and D_2 has been reported separately by C. H. Church as Technical Report No. 1 (ASTIA AD-211110) under this contract. The abstract from that report is given here as a résumé of the work.

ABSTRACT OF TECHNICAL REPORT NO. 1

A high-resolution study has been made of the electric field induced vibration-rotation absorption spectra of H_2 and D_2. The induced absorption was modulated at 90 cps by square wave fields of 100,000 volts/cm maximum value applied to a one-meter-long Stark cell of the light-guide type operated at pressures up to 30 atmospheres. The spectrum was analyzed by a F/15 vacuum grating spectrograph of the Ebert design using a 200-mm-wide grating with 300 lines per mm double-passed. The radiation was detected by lead sulfide photoconductive cells cooled by liquid nitrogen. The small modulated component of the output of the detector was isolated and amplified electronically. White light fringes produced in a Fabry-Perot etalon were used for the determination of the line positions. The absolute intensities of the lines were measured for specific polarization directions to calculate the polarizability components of the molecules. The spectral resolution varied between 0.1 and 0.2 cm^{-1}. The probable error in the determination of the transition frequencies was 0.02 cm^{-1}, and that for the values of the polarizability components was 3%.

The ν_{0-1} transitions observed for H_2 included 6 Q branch lines, 4 S lines, and 1 O line that was largely obscured; and the ν_{0-2} transitions, 3 Q lines. For D_2, 5 Q and 5 S lines were detected in the fundamental, and 3 Q lines in the overtone. The spectral resolution used (0.1 to 0.2 cm^{-1}) was comparable to the line widths. A new set of molecular constants was calculated for both H_2 and D_2 to fit the data best, generally within 0.01 cm^{-1}. They differed only slightly from those given by Stoicheff. The ratio of the equilibrium vibrational frequencies of H_2 and D_2 could not be compared closely with the ratio determined by the reduced masses of the molecules because of the lack of a reliable value of ν_{0-3} for D_2. The values obtained for the polarizability matrix elements α_{01} and γ_{01} for both molecules are in excellent agreement with the most recent experimental determinations from static electric field induced absorption and photoelectric Raman and Rayleigh scattering data.

It is concluded that the modulated electric field absorption technique offers the highest sensitivity in the detection of weak vibration-rotation transitions in H_2 and D_2, and yields values of line positions and intensities

of comparable or greater accuracy than other available methods. Several changes are suggested that should further improve the technique.

An attempt was made to detect a possible shift of the line position due to the applied electric field. The most sensitive method for sensing such a shift appeared to be modulation with a square wave field between the values E and $E \times 2^{-1/2}$. The intensity of the absorption is proportional to E^2, and a shift of the frequency would also be expected to have the same dependence. The difference signal would then be half of its usual strength due to the first factor, and the line shape would be asymmetric due to the second. Most of the tests were made on the Q_1 (1) line of H_2 because of its strength. However, no trace of asymmetry in the line shape was evident. It was estimated that a shift of 0.01 cm^{-1} would have been observable.

V. STARK EFFECTS IN THE VIBRATION-ROTATION SPECTRA OF POLAR MOLECULES

Stark first showed that the Balmer lines of hydrogen when excited in a strong electric field were split into a number of components.[12] Since then the Stark effect has become a standard aid in the analysis of spectra not only of electronic transitions of atoms but also of rotational transitions of polar molecules in the microwave region. Stark effects in the vibration-rotation lines of H_2O and NH_3 were noticed by Terhune and Peters,[13] but the gas pressure of 10 atmospheres necessary to prevent breakdown of the gas in the high electric field (70,000 volts/cm) produced absorption lines too broad to be interpreted with any confidence.

It was possible to make a substantial improvement in the observation of Stark effects with the equipment used for the induced absorption in H_2 and D_2 discussed in the previous section. The relevant features were a 36-in.-long absorption cell between flat parallel polished metal electrodes with a separation of about 1.5 mm, a square wave 90-cps voltage supply sufficient to produce fields of more than 100,000 volts/cm, and a 3-meter Fastie-Ebert double-passed grating monochromator. The difference signal between absorption with the electric field off and on at the 90-cycle rate was recorded. Several representative spectra are shown in the accompanying figures. In Fig. 11, the normal absorption of 1 cm of NH_3 buffered with 24-cm pressure of N_2 is given on the lower trace and the Stark difference signal with a square wave field of 10,000 volts/cm on the upper trace near the center of the symmetric N-H stretching frequency. The Stark difference signal is sensitive to the polarization of the incident radiation as shown in Fig. 12. Here parallel and perpendicular refer to the relative directions of the electric vector of the radiation to the direction of the applied electric field. In the parallel orientation, transitions having $\Delta m = 0$ are singled out; in the perpendicular case, $\Delta m = \pm 1$.

The frequency shifts of the energy levels of NH_3 are proportional to the square of the electric field strength, whereas a symmetric top molecule not having inversion doubling will show a linear Stark shift which in general should be larger—other factors such as the dipole moments being similar. Methyl fluoride is such a case, and the normal absorption and Stark difference signals are shown in Fig. 13 for 1 cm of CH_3F with 5 cm of N_2, E = 6500 volts/cm, in the high-frequency wing of the perpendicular band involving the asymmetric C-H stretching motion. The final example, Fig. 14, is the first overtone of CO. Since the dipole moment of CO is small (0.1 debye) and the overtone absorption weak, a high pressure (2 atmos. CO with 9 atmos. of H_2) and high field (85,000 volts/cm) are needed to produce an appreciable signal.

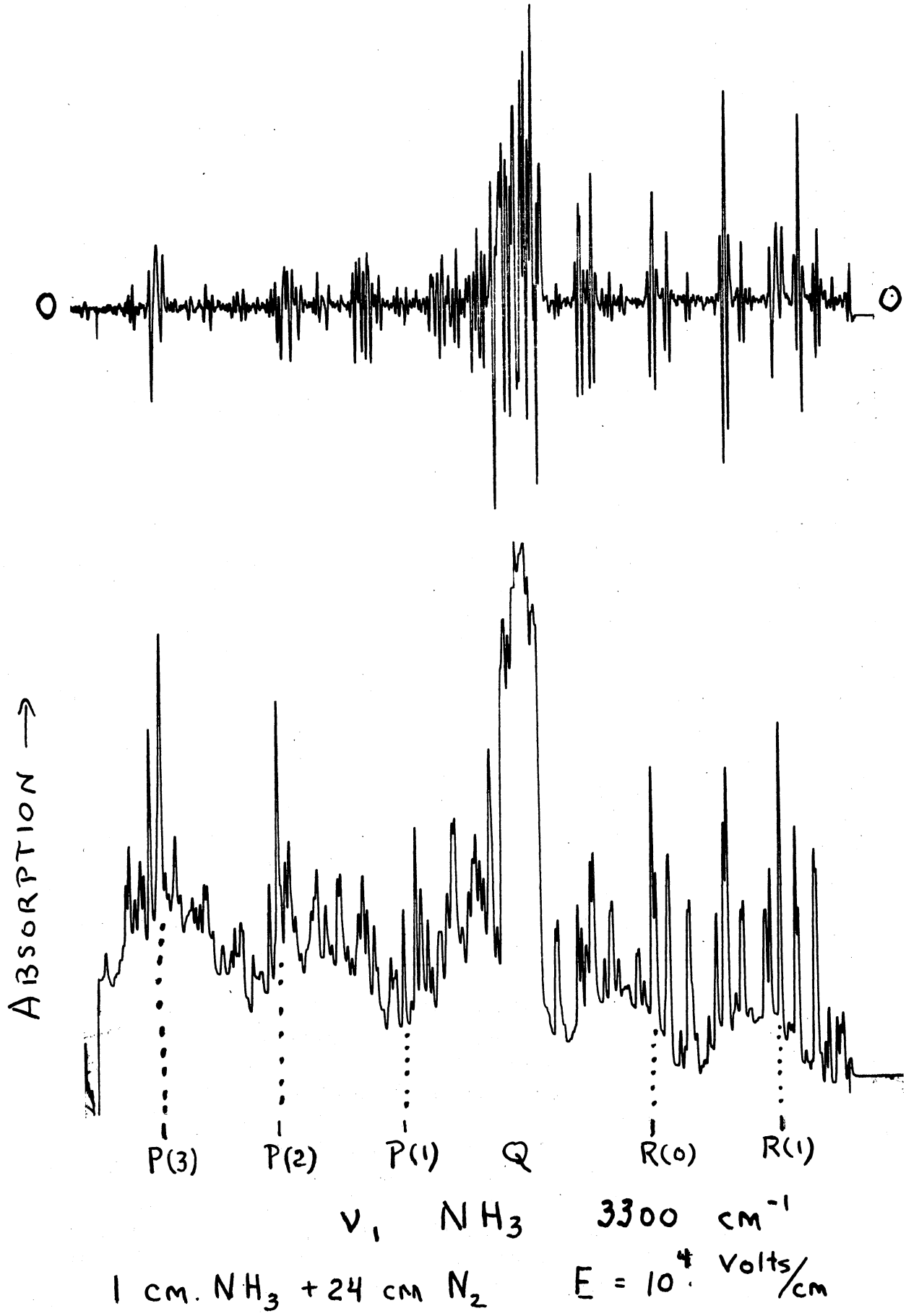

Fig. 11. Above: Stark difference signal near center of ν_1 band of NH_3 at 3300 cm^{-1}. 1 cm NH_3 + 24 cm N_2, square wave field of 10^4 volts/cm. Below: Normal absorption, same conditions except no field.

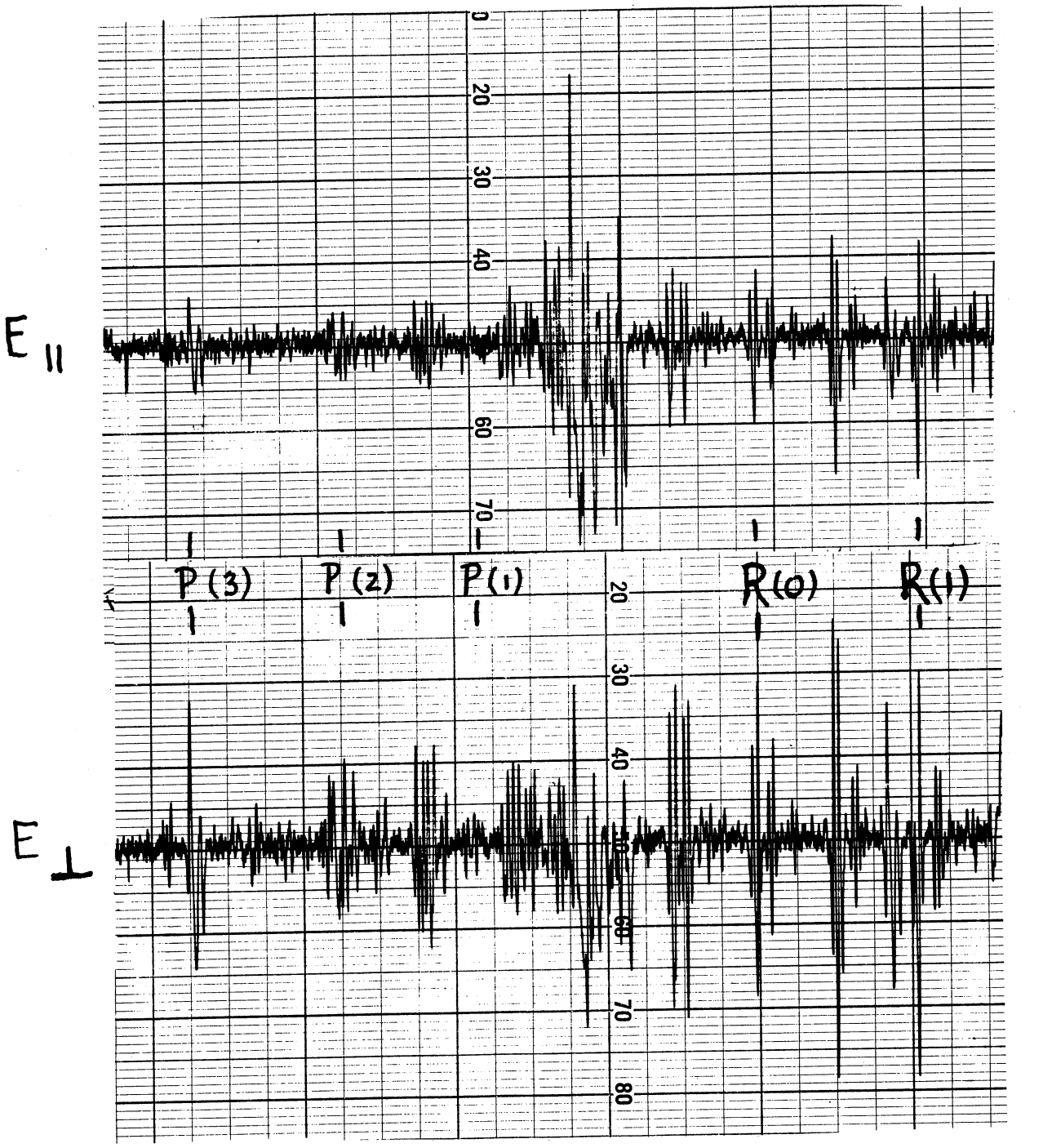

Fig. 12. Polarized Stark difference signals for ν_1 of NH_3; 1cm NH_3 and 25 cm N_2; E = 10^4 volts/cm. Above: Parallel polarization ($\Delta m = 0$). Below: Perpendicular polarization ($\Delta m = \pm 1$).

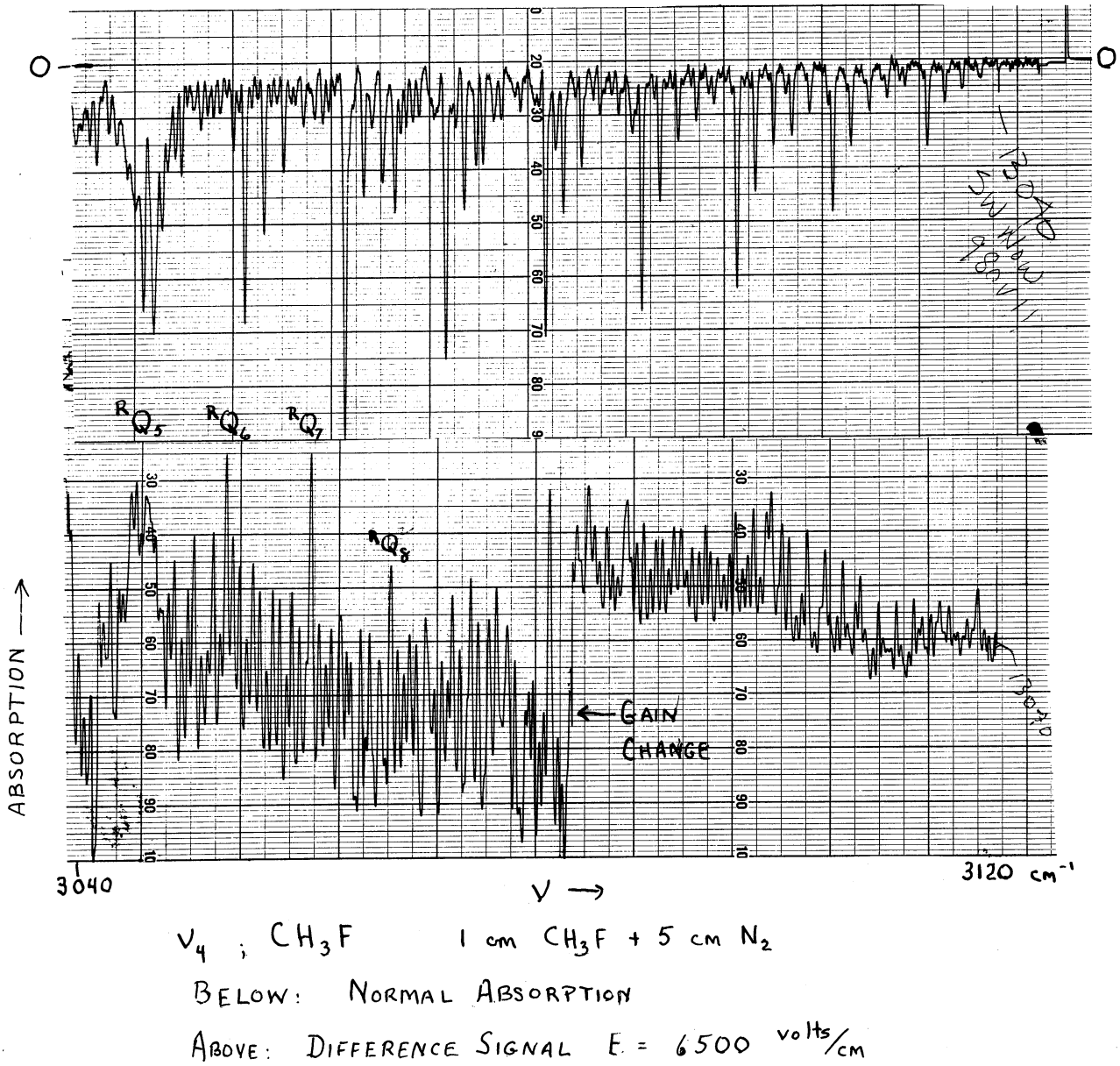

Fig. 13. Normal absorption (below) and Stark difference signal (above) for part of ν_4 of CH_3F; 1 cm CH_3F + 5 cm N_2; E = 6500 volts/cm.

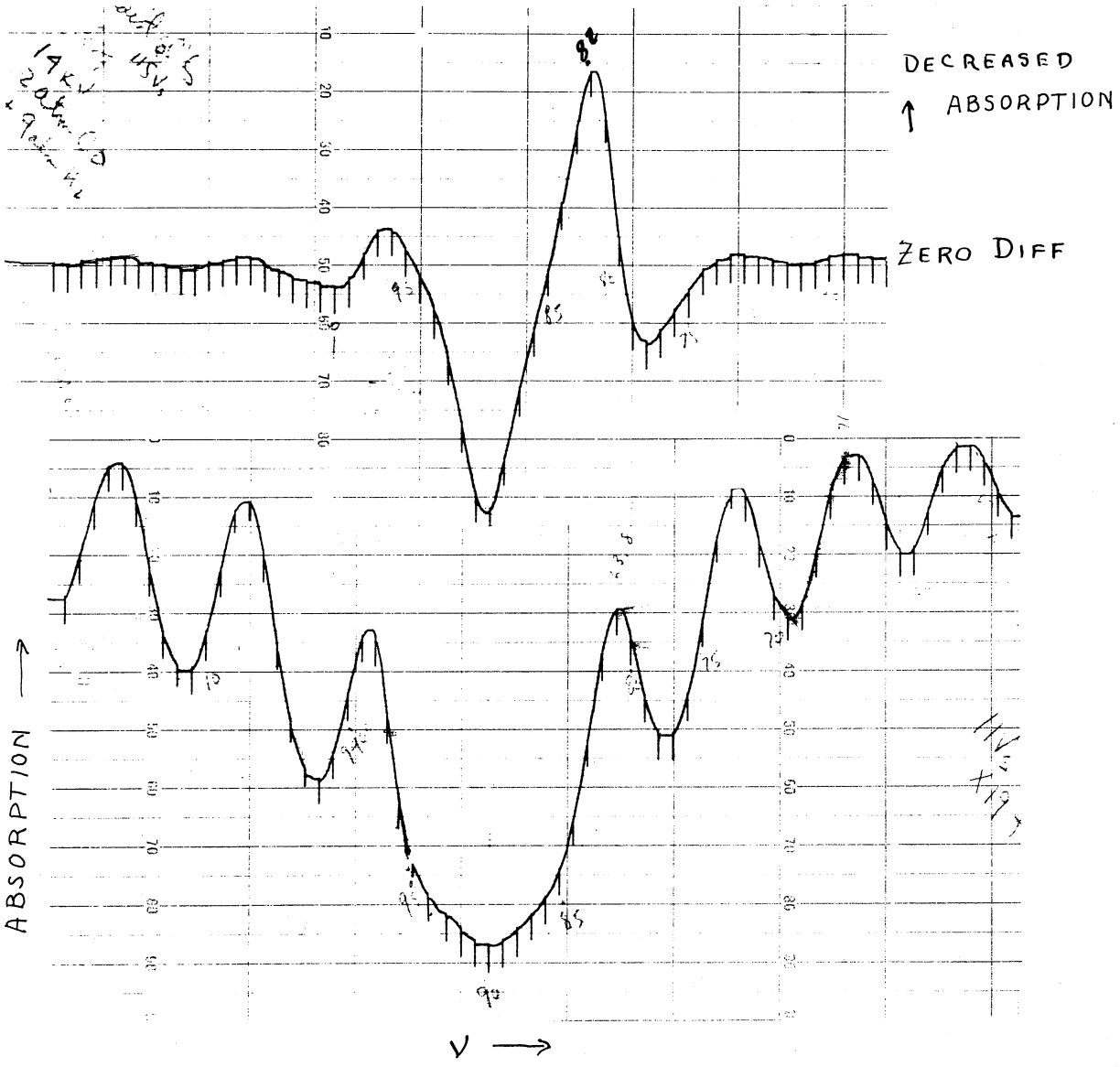

Fig. 14. Normal absorption (below) and Stark difference signal (above) for CO overtone near 4400 cm^{-1}; 2 atmos. CO and 9 atmos. H_2; E = 85,000 volts/cm.

At this time we learned that C. C. Costain at the National Research Council of Canada had achieved field strengths of several hundred thousand volts per cm with small electrode separation as well as low gas pressures in an attempt to find induced rotational absorption of nonpolar molecules in the microwave region. Considerable care had to be exercised to remove the last dust specks that would otherwise initiate a breakdown spark across the gap. As an example, the breakdown voltage vs. the product of pressure in mm of Hg and the separation in mm of plane parallel electrodes is given in Fig. 15. From this plot it can be seen that for a 0.25-mm gap and 4-mm pressure of CO_2 (sufficient for strong absorption in a meter path), the breakdown voltage would be approximately 1500 volts and the corresponding field strength 60,000 volts/cm.

Considerable difficulty was experienced in making satisfactory cells, chiefly with regard to breakdown voltage, transmission of the infrared radiation, and uniformity of the spacing. The most successful method of construction to date has been to use the best quality 1/4-in. plate glass for electrodes, each 36 x 2-1/2 in., with the inner surface of each coated with an evaporated metal film to within 1 or 2 mm of the edges. Spacer strips were made of Mylar, 10 mm wide and 0.25 mm thick. A strip of 1 mil Lufkin feeler gauge stock was placed between the top Mylar strip and one electrode and another between the bottom Mylar strip and the other electrode, and the electrical leads were soldered to these metal strips. The electrodes and spacers were assembled between 2 pieces of ground channel iron under slight pressure and then connected together along the lengthwise seams with Araldite epoxy resin. It was found that the evaporated films could be made partially transparent without seriously affecting the lengthwise transmission of infrared energy. Thus, interference fringes could be observed looking perpendicularly through the plates at a fluorescent lamp and the uniformity of the separation of the electrodes determined. In some cases, 90% of the area was parallel to within ± 2 fringes of yellow light. The absolute spacing of the electrodes was measured by inserting the cell transversely in the beam of the spectrometer and measuring the spacing of the channelled spectrum fringes from which the separation could be calculated to a fraction of a percent accuracy.

When the Stark cell was in use, the infrared energy was focused on its far end at F/60, so that the rays at the extreme angle to the optic axis were less than 1/2° from grazing reflection. The slight difference in the reflectivity of the evaporated metal film for the two orientations of the electric vector of the radiation led to an appreciable polarization of the transmitted radiation for 0.25-mm gap cells. Since the slit width of the F/15 spectrometer was of the order of 0.05 mm, the radiation leaving the Stark cell was demagnified 4 X, but had to be imaged very carefully. The curved Ebert slit neccessitated an oblique reflection from a curved surface at an intermediate focus to match the straight "slit" of the Stark cell. Over-all transmissions of 10 to 20% were obtained for 0.25-mm cells, and 40 to 50% for 0.5-mm cells in the arrangement.

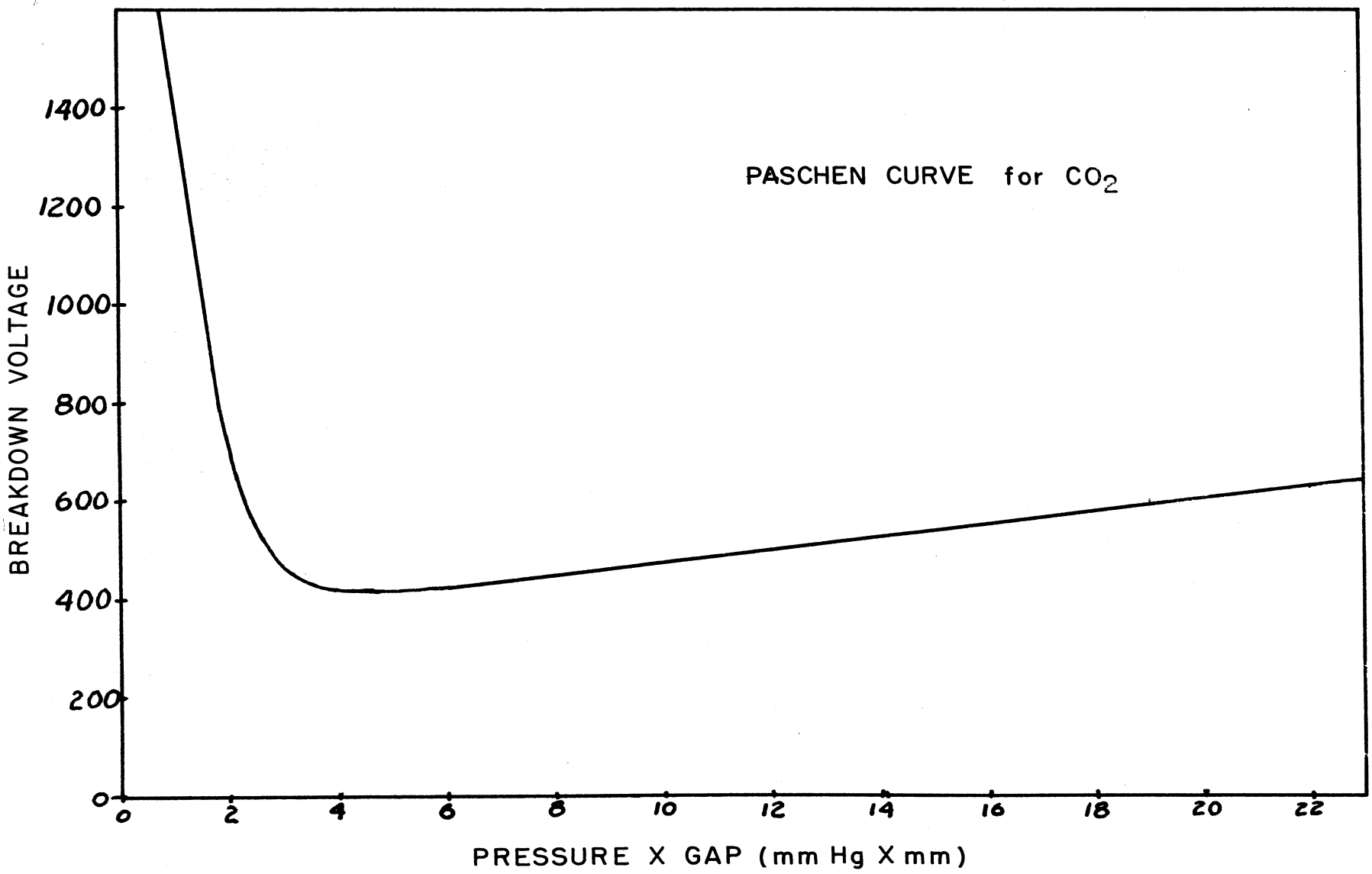

Fig. 15. Breakdown voltage vs. pressure x gap for CO_2.

The breakdown voltages of these cells were considerably below the published values for optimum conditions. This has been attributed to dirt specks and the like that initiate the discharge. Some cells have been operated at 120,000 volts/cm, although in general 70,000 volts/cm is the usually attainable maximum if the pressure is no more than 1 mm of Hg.

The results are reported here on several representative molecules—principally HCN and CH_3F, although some observations on NH_3 and H_2O are also included. All these molecules possess large dipole moments of the order of 1 debye or more. Their Stark effects are determined primarily by their rotational motion, and the effects of the vibration enter only as small changes due to the change in dipole moment with vibration state and the change in the moment of inertia with vibrational state. Any effect due to the polarizability of the molecule is negligible by comparison at the electric field strengths presently used. A perturbation calculation of the Stark effect of symmetric top molecules through fourth-order terms has been carried out by Dr. K. T. Hecht and is repeated here.

μ : dipole moment
E : electric field strength
W : energy of the state
B : rotational constant
J : total angular momentum
K : component of J along figure axis of molecule
M : component of J in the direction of the electric field

1. HCN.—For a linear molecule, such as HCN, $K \equiv 0$; so that the first-order or linear term is always zero and the molecule shows a quadratic Stark effect for small fields or rather for small values of $\lambda\left(\lambda \equiv \frac{\mu E}{B}\right)$. HCN was selected for study because of its favorable values of μ_o (2.96 debye) and B_o(1.478 cm^{-1}) as well as the fact that its C-H stretching frequency at 3311 cm^{-1} is in a convenient region of the spectrum. The energy shifts of the lower J states can be quite large as shown in Fig. 16, where, for example, the P(1) line is shifted nearly 1 cm^{-1}. As J increases, the difference of the shifts of the ground and excited vibration-rotation levels between which transitions are allowed becomes progressively smaller. The weaker components of the transitions between the Stark shifted levels are obscured to a certain extent by the components of "hot" bands—2 sets of which can be recognized in the normal absorption trace at the bottom. These "hot" bands show a somewhat different Stark effect from that of the fundamental because of their vibrational angular momentum. An attempt to observe the individual components for the R(0) and P(1) lines of these "hot" bands were fruitless because their intensities was too weak. Thus the inability of the present apparatus to observe weak transitions is a serious limitation.

SYMMETRIC TOP STARK EFFECT
FOURTH-ORDER PERTURBATION CALCULATION

$$\lambda = \mu E/B \qquad \epsilon = W/B$$

$$\epsilon = \epsilon_o - \lambda \frac{KM}{J(J+1)}$$

$$+ \lambda^2 \frac{J^3(J+1)^3 - 3(M^2+K^2)J^2(J+1)^2 + M^2K^2[5(J^2+J) + 3]}{2J^3(J+1)^3(2J-1)(2J+3)}$$

$$-\lambda^3 \frac{KM[5J^4(J+1)^4 - (M^2+K^2)J^2(J+1)^2(7J^2+7J+6) + M^2K^2(9J^4+18J^3+28J^2+19J+6)]}{2J^5(J+1)^5(J-1)(J+2)(2J-1)(2J+3)}$$

$$+\lambda^4 \text{ (fourth-order term)}$$

Except for the special cases:

$$J = 1, \quad |K| = |M| = 1, \quad \epsilon = \epsilon_o - \lambda \frac{KM}{2} - \lambda^2 \frac{3}{80} + \lambda^3 \frac{3KM}{960} - \lambda^4 \frac{89}{2,688,000} .$$

$$J = 0, \quad K = M = 0, \quad \epsilon = \epsilon_o - \lambda^2 \frac{1}{6} + \lambda^4 \frac{11}{1080} - \lambda^6 \frac{1}{725} .$$

SYMMETRIC TOP STARK EFFECT
FOURTH-ORDER PERTURBATION CALCULATION

$$\text{Fourth Order Term} = \frac{1}{8(2J-1)^3(2J-3)(2J+3)^3(2J+5)} \times$$

$$\left[(20J^2+20J+33) - \frac{18(M^2+K^2)(28J^2+28J-5)}{J(J+1)} + \frac{9(M^2+K^2)^2(68J^4+136J^3+125J^2+57J-45)}{J^3(J+1)^3} \right.$$

$$\left. \times \left[+ \frac{1}{(J-1)(J+2)J^3(J+1)^3} \left[2M^2K^2(2052J^6+6156J^5+4885J^4-490J^3-4292J^2-3021J+1710 \right. \right. \right.$$

$$\left. \left. \left. - \frac{2M^2K^2(M^2+K^2)}{J^2(J+1)^2} \quad 2860J^8+11440J^7+19539J^6+18577J^5 \right. \right. \right.$$

$$\left. \left. \left. -92J^4-17799J^3-9522J^2+567J+2430 \right. \right. \right.$$

$$\left. \left. \left. + \frac{M^4K^4}{J^4(J+1)^4(J+2)} \quad 5876J^{11}+41132J^{10}+134009J^9+275214J^8+355474J^7 \right. \right. \right.$$

$$\left. \left. \left. +217100J^6-58250J^5-194746J^4-125274J^3 \right. \right. \right.$$

$$\left. \left. \left. -8775J^2+22140J+8100 \right. \right. \right] \right]$$

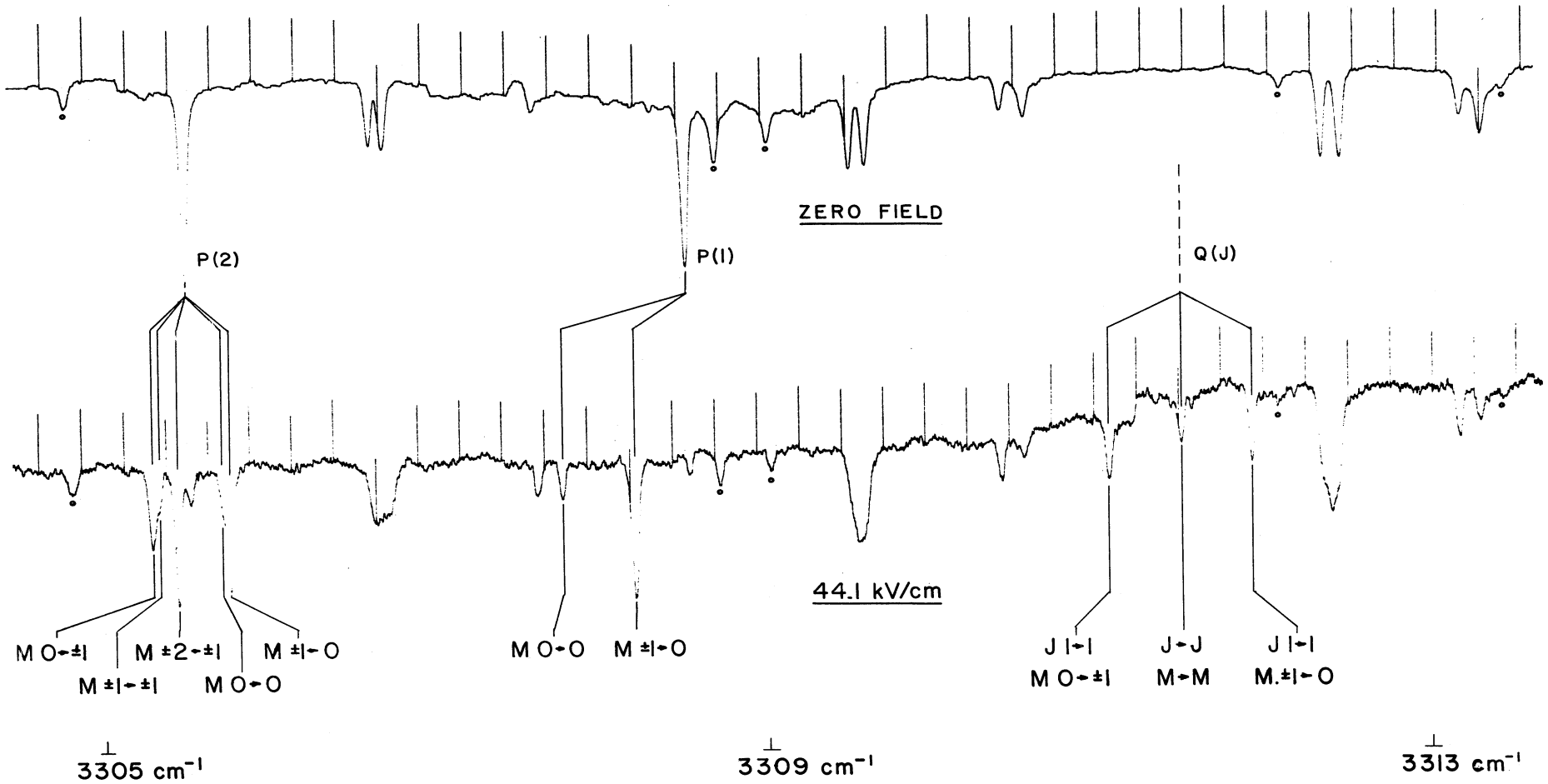

Fig. 16. Above: Zero field absorption of P(1) and P(2) lines of ν_3 of HCN. Below: Stark spectrum of same region, E = 44,000 volts/cm.

The line shifts may be used to calculate the magnitude of the dipole moment in both the ground and excited vibrational states. In the case of Fig. 16, $\lambda = \frac{\mu E}{B} \gg 1$, and λ is so large that a perturbation calculation is no longer valid. An exact solution for such cases has been given by Lamb and has been evaluated by Kusch and Hughes.[14] For the excited vibrational state, there has been a change in λ of $\Delta\lambda = \lambda\left(\frac{\Delta\mu}{\mu} - \frac{\Delta B}{B}\right)$. Referring to Fig. 17 where the approximate dependence of J = 0 and 1 on λ for the two vibrational states are indicated, the $\Delta m = 0$ component of the R(0) line would be represented by a slightly off-vertical transition from "a" to "c'," and the $\Delta m \pm 1$ component by the transition from "a" to "b'." Similarly, $\Delta m = 0$ of P(1) would be represented by going from "c" to "a'," and $\Delta m = \pm 1$ of P(1), from "b" to "a'." It is then evident, for example, that the separation of the $\Delta m = 0$ and $\Delta m = \pm 1$ components of R(0) gives directly the m splitting of the J = 1 excited vibrational state, and knowing E and B excited, λ excited and thence μ excited can be found from the data of Kusch and Hughes. In this way, the dipole moment in the first excited vibrational state of ν_1 of HCN is found to be 2.99 as compared to the ground state value of 2.96 debyes determined by microwave measurements. It turns out to be more accurate to determine the change in the dipole moment from the difference in the separation of b-c and b'-c'. The limiting factor in the precision is the nonuniformity of the grating drive at the present time.

In addition, the perturbation of the electric field in producing an interaction of the energy levels, mixes the original wave functions, so that J is no longer an exact quantum number, or correspondingly the $\Delta J = 0$ selection rule no longer holds strictly. There are three weak components observable near the center of the band which presumably arise from the J = 1 levels, since the perturbation and consequent intermixing of the higher J states falls off rapidly. The central component is evidently the superposition of M $0 \rightarrow 0$ and $\pm 1 \rightarrow \pm 1$; the low-frequency component, M $0 \rightarrow \pm 1$; and the high-frequency one, M $\pm 1 \rightarrow 0$.

2. CH_3F.—Only symmetric top molecules regularly show a Stark effect linearly proportional to the applied field. Methyl fluoride was taken as a representative case primarily because fluorine has only one stable isotopic form. Its large dipole moment of 1.79 debyes permits observation of the Stark shifts at moderate fields (as in Fig. 13), but its small value of B of 0.85 cm^{-1} coupled with the K structure of the bands produces a spectrum of many closely spaced lines. With the available resolution in the infrared it is nearly impossible to separate the Stark components of a particular line in these circumstances. However, in obtaining a Stark difference signal by modulating the electrodes of the cell with a 90-cps square wave voltage of moderate magnitude, the components are not resolved, but the signal, resulting from the broadening of a line, is proportional to the frequency shifts calculated for the particular values of J, K, and M involved in the transition. For electric field strengths small enough that the first-order term of the perturbation calculation is dominant, the components are symmetrically shifted

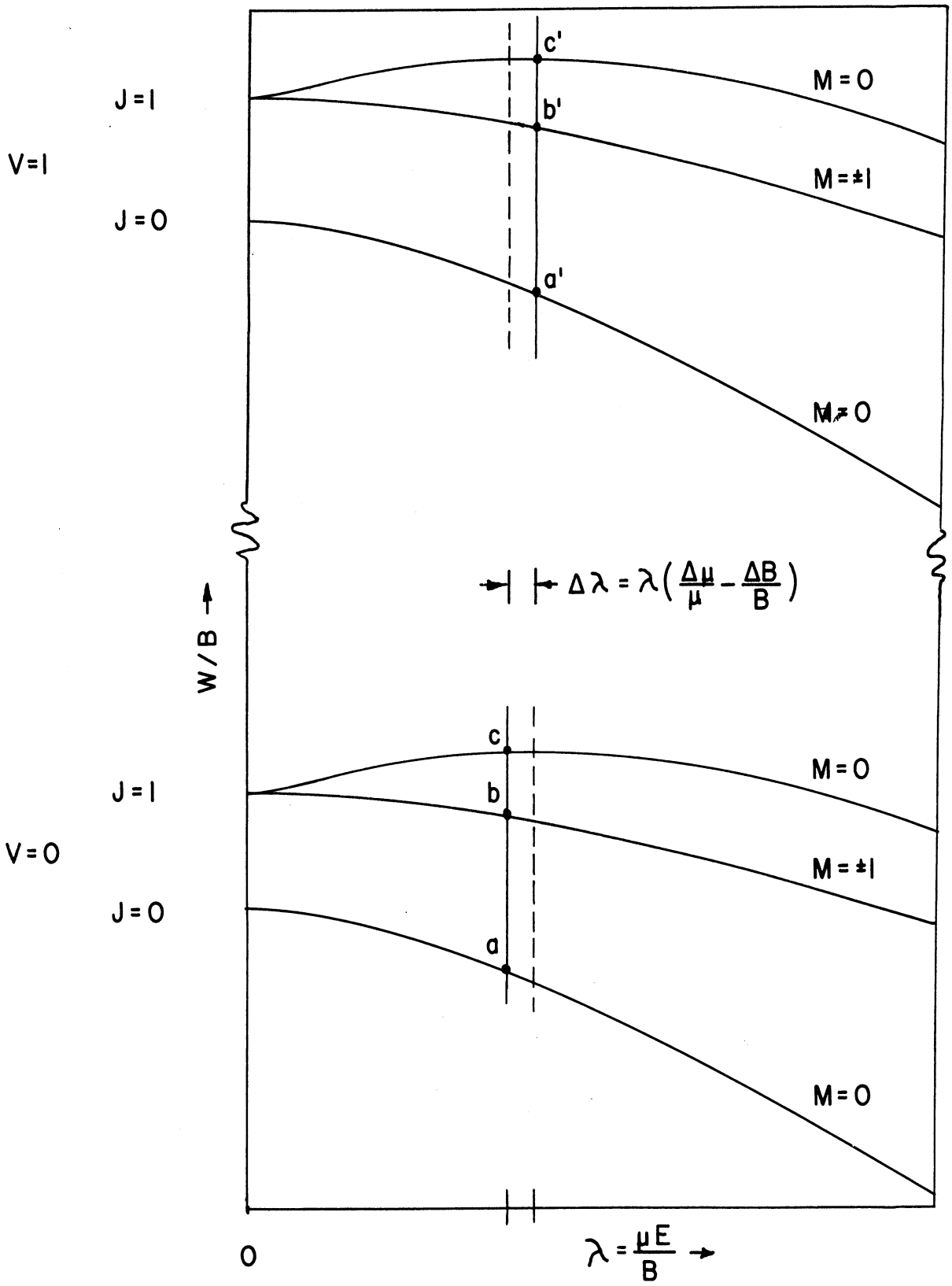

Fig. 17. Energy levels of a vibrating linear molecule in an external electric field.

with respect to the original line position. In scanning a line, the resultant output of the amplifier having phase sensitive rectification would be as indicated in Fig. 18, in which the areas of increased absorption would equal the areas of decreased absorption only if the absorption is in the linear range. The net effect of the electric field modulation is further modified by overlapping of the absorptions of individual lines.

The normal absorption and the electric-field modulated spectra of a high-frequency portion of the asymmetric C-H stretching fundamental, ν_4, of CH_3F (a perpendicular type band), are shown in Figs. 19 and 20. Effectively the spectrum is simplified or rather additional contrast between lines is produced by the Stark modulation. This results from the fact that the difference in frequency shifts in the ground and excited states related by $\Delta m = 0$ or ± 1 (and hence the line broadening), varies approximately inversely as J for given K states. This additional weighting factor causes a rapid diminution of intensity of transitions between the higher J levels, and the origin of the R branch lines of the several K subbands stand out clearly as noted on the figures. The extra clue is enough to initiate a rapid unraveling of the band structure. For example, by counting the number of missing lines from the terminus of the R branch to the Q branch, one can make a positive identification of the K values of a particular subband. In addition a perturbation of the line spacing, as occurs in the K $4 \rightarrow 5$ subband is readily recognized.

The Stark modulated signal in an extreme case of a molecule whose rotational lines from the various subbands are so close together as to produce nearly continuous absorption may introduce enough variation of signal strength between adjacent lines to yield a measurable spectrum. This is nearly the situation in the same ν_4 band of CH_3I. In the normal absorption trace of Fig. 21, it is difficult to assign the individual lines, whereas the emphasis of the Stark spectrum on the low J states permits one to make an unambiguous assignment.

The spectra of parallel-type bands of these molecules lies in a much smaller frequency range because of the $\Delta K = 0$ selection rule for such transitions. For a particular change in J, there is usually some shift in the energy for different K values due to the change of A and B with the vibrational state. Adjacent lines in the spectrum ordinarily then have nearly the same values of J and also K, so that their Stark effect broadening is approximately the same. The exception occurs for lines involving the $K = 0$ state, for which the Stark shift is zero. This may be used as a criterion for the identification of the $K = 0$ components as shown in the case of the symmetric C-H stretching fundamental ν_1 of CH_3I in Fig. 22. The K splitting in the R and Q branch lines near the band center is appreciable. The application of a d-c electric field spreads out the M components of all lines not having $K = 0$ and reduces their peak absorption. The unaffected lines can then be readily identified as the $K = 0$ components, as for example $R(0)_{K=0}$, $R(1)_{K=0}$ and $R(2)_{K=0}$ in Fig. 22.

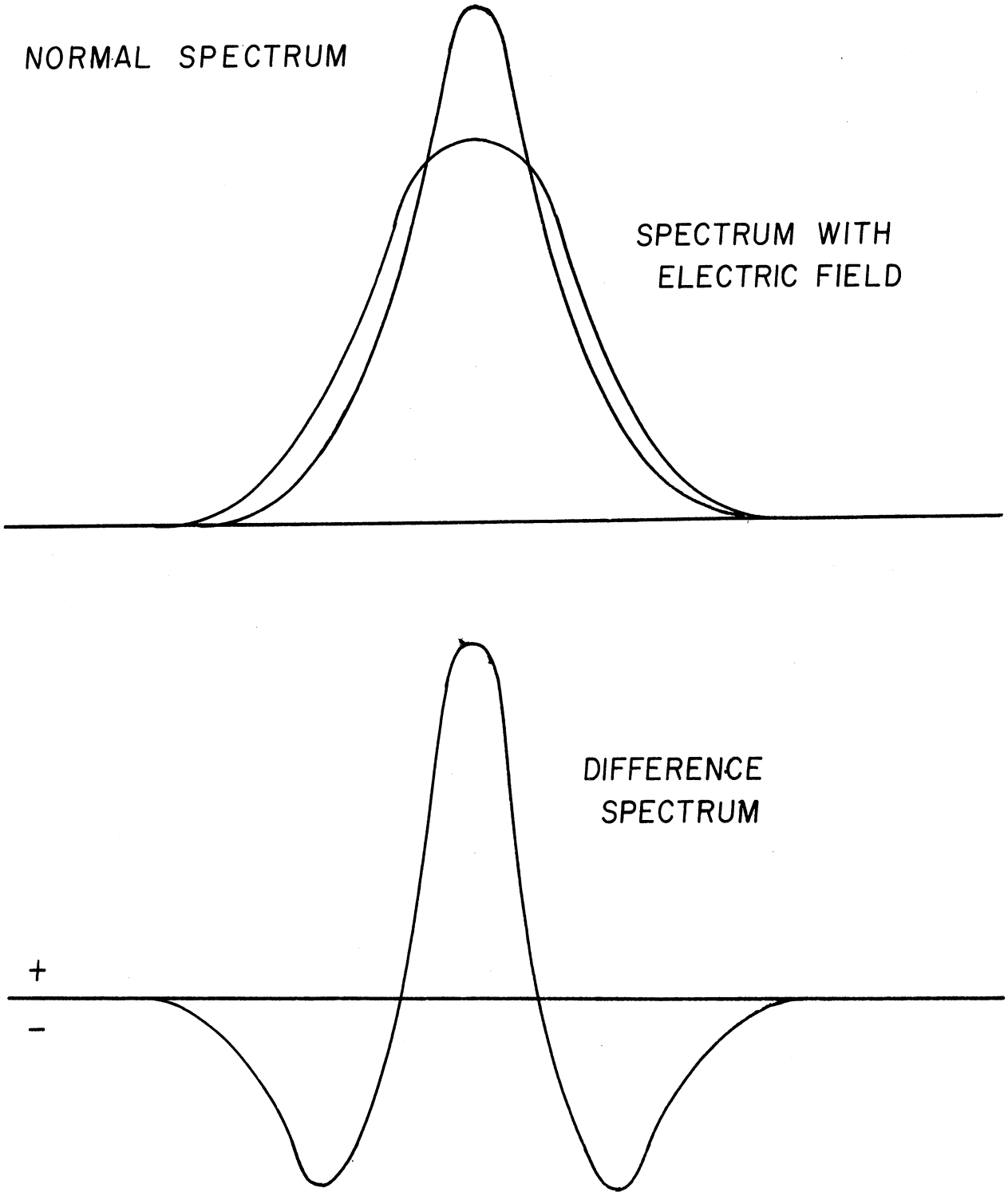

Fig. 18. Illustration of the Stark difference-spectrum arising when the individual Stark components are symetrically displaced but are unresolved.

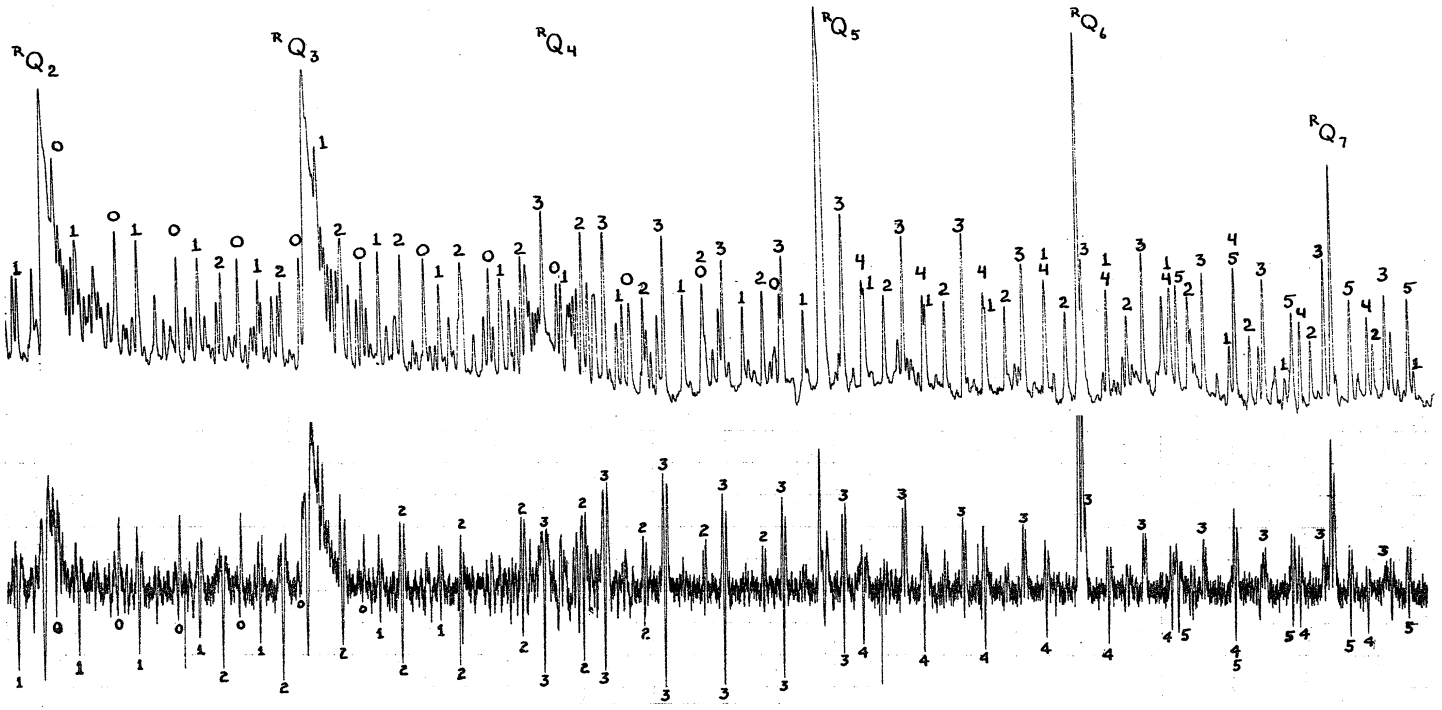

Fig. 19. R lines of R subbands of ν_4 of CH_3F. Above: Normal absorption. Below: Stark difference signal, 12,000 volts/cm.

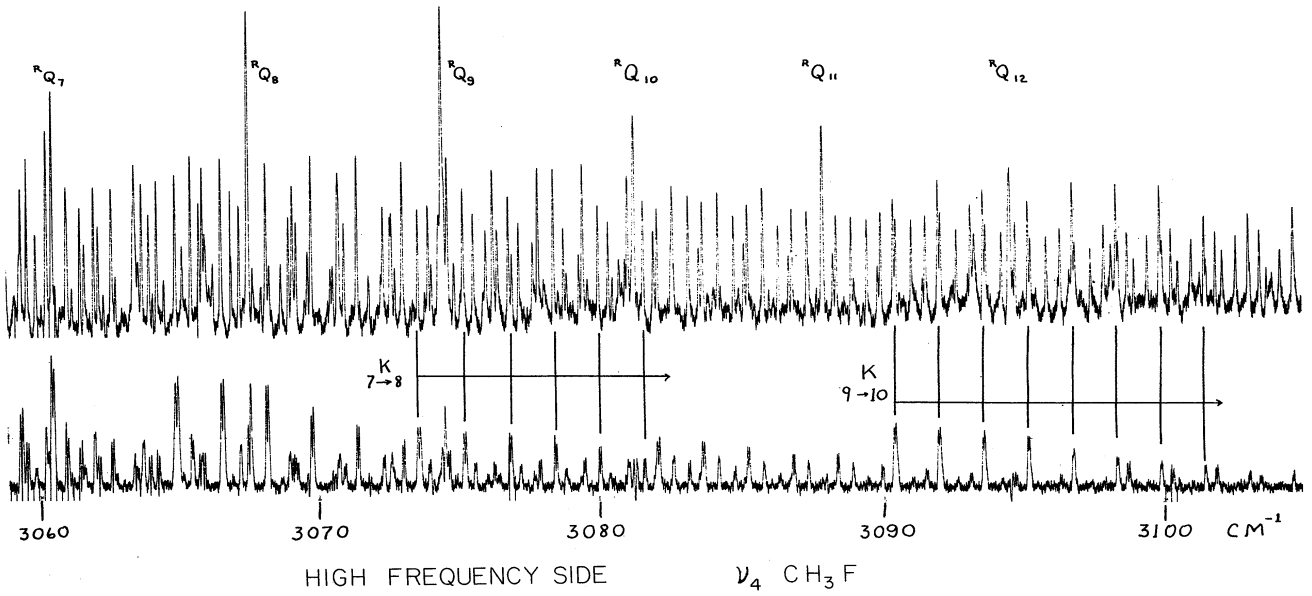

Fig. 20. High frequency side of ν_4 of CH_3F, 3 mm pressure. Above: Normal absorption. Below: Stark difference signal.

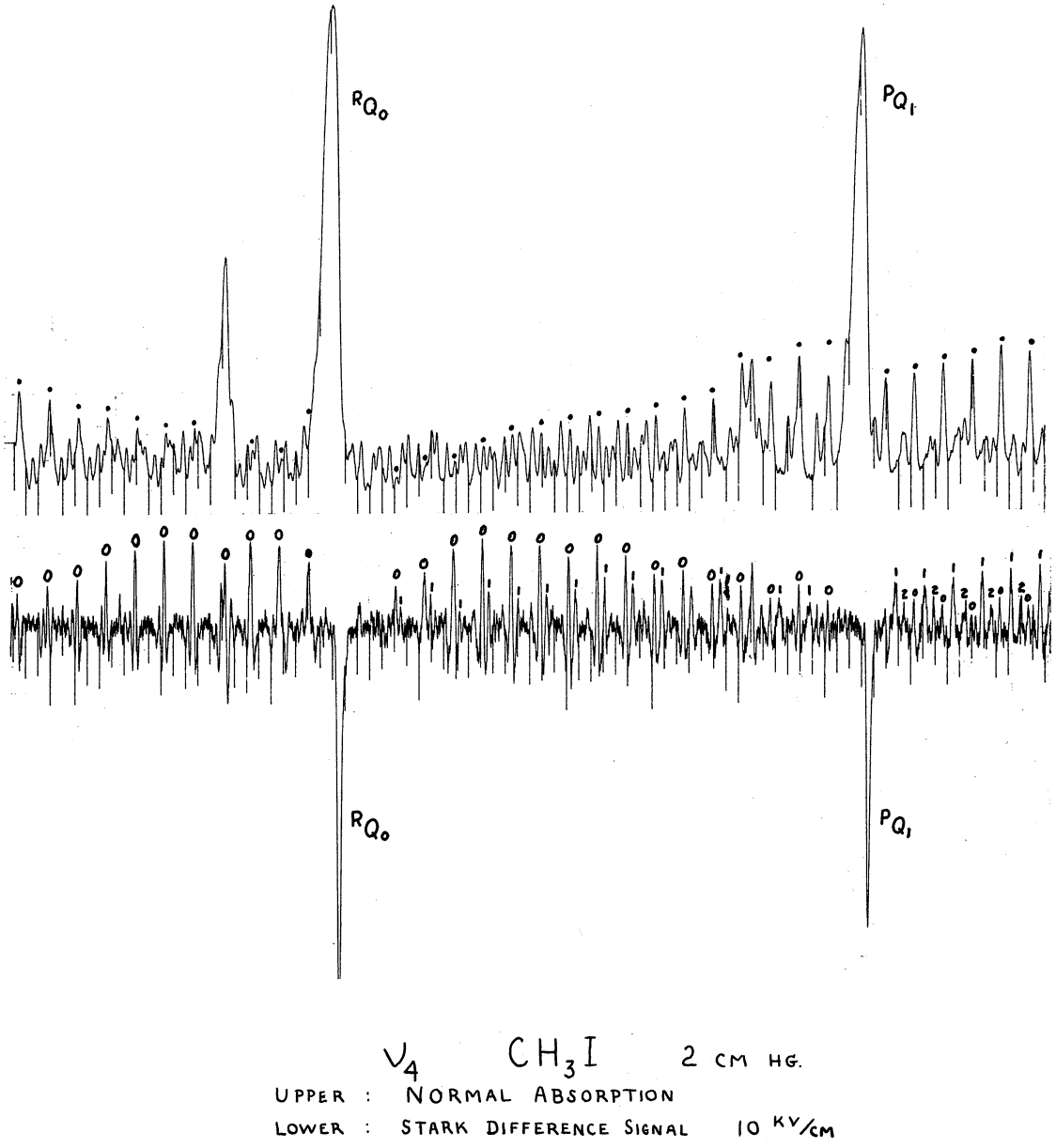

Fig. 21. ν_4 of CH_3I, 2 cm pressure. Above: Normal absorption. Below: Stark difference signal, E = 10^4 volts/cm.

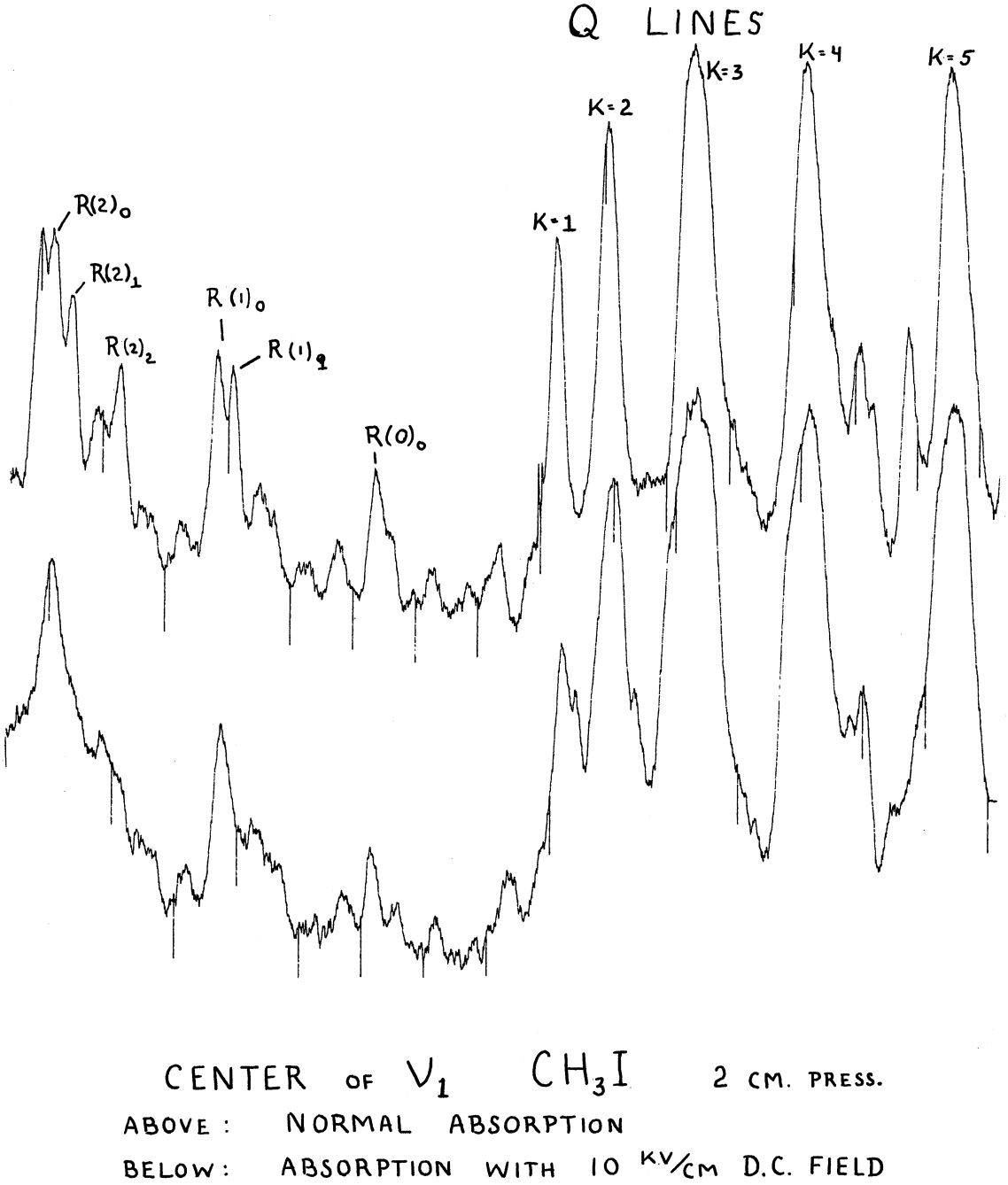

Fig. 22. ν_1 of CH_3I, 2 cm pressure. Above: Zero field absorption. Below: Absorption with 10^4 volt/cm d-c field.

With the origin of a particular R(J) set established, the other K components can be recognized by their nearly quadratic spacing.

Through the use of these several clues furnished by the Stark effect, a complete identification has been made of the rotational fine structure of the ν_1 and ν_4 fundamentals of CH_3I with relative ease. In CH_3F, the similar vibrations overlap and furthermore interact. Consequently the assignment of the rotational lines is a more formidable task and has been only partially completed to date—perhaps two-thirds of the total number of lines identified with assurance.

3. NH_3.—The inversion property of the ammonia molecule removes the K degeneracy of a symmetric top which otherwise leads to a linear Stark effect. However, the Stark effect may be used to measure the inversion splitting in both the ground and the excited vibrational states as a function of the rotational quantum number J. In Fig. 23, the normal absorption of the J 1→2 rotational transition in ν_1 of NH_3 near 3380 cm^{-1} shows the several K components resolved (the weak periodic variation in intensity is due to interference effects in the windows of the spectrometer). The Stark difference signal above is due entirely to the K = 1 components, since there is no shift of a K = 0 level. From the polarity of the signal, it is determined that the lines move apart when the field is applied. In addition, two weak absorption lines now appear midway between the two K = 1 components. These two new lines are dependent on the electric field strength. As the field increases, their separation at first decreases until they appear to cross over at the center of gravity of K = 1 components, and then rapidly diverge—meanwhile increasing in absorption strength. Referring to the energy level diagram of Fig. 24, showing the inversion splittings of Δ_0 and Δ_1 in the ground and excited states, the selection rules permit only the two transitions shown if no field is present. Hence the separation of the K = 1 components of 1.78 cm^{-1} in the normal spectrum is the sum of Δ_0 and Δ_1. The electric field splits the levels as shown on an exaggerated scale, but the perturbation intermixes the wave functions of all but the m = 0 states. In terms of the symmetries of the states with respect to inversion, there will now be weak transitions possible between "s" states and also between "a" states, as indicated by the dashed lines, in addition to the usual ones. As predicted by theory, the Stark shift in the ground state ϵ_0 is larger than that in the excited state ϵ_1—both being proportional to E^2. Considering radiation polarized parallel to the applied electric field so that $\Delta M = 0$, the new transitions are from M = 1 to 1, and their frequency difference is $\Delta_1 - \Delta_0 + 2(\epsilon_1-\epsilon_0)$. The field dependence of these induced transitions noted earlier rests in the $(\epsilon_f-\epsilon_0)$ term. Finally, the separation of the two lines extrapolated to zero field gives directly the difference in the inversion splittings of the states. This coupled with the sum of the inversion splittings available in the normal spectrum yields values of both Δ_0 and Δ_1. (The intepretation of the perpendicular polarization ($\Delta m=\pm 1$) closely follows the above but is more involved.)

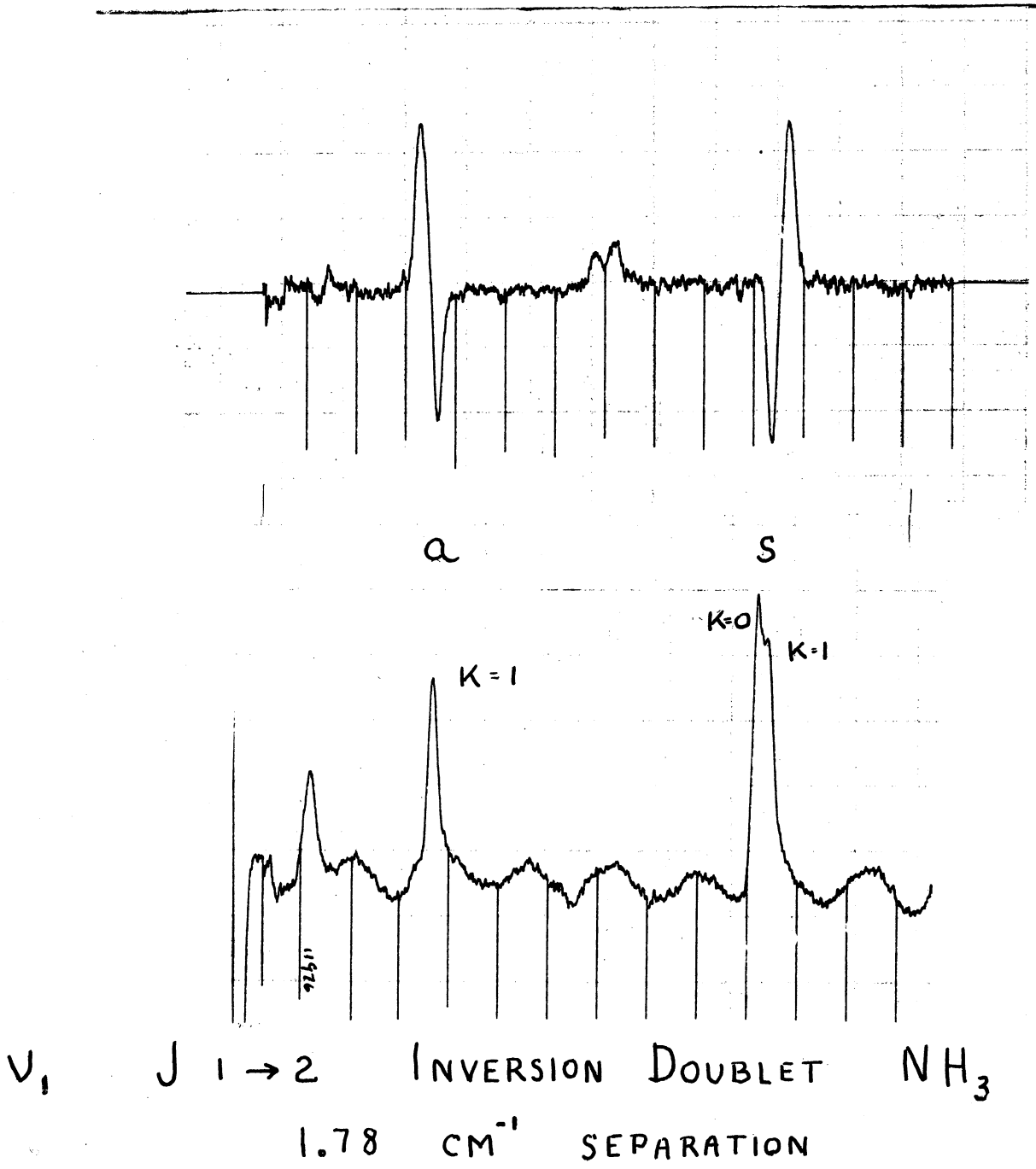

Fig. 23. J 1 → 2 inversion doublet of ν_1 of NH_3, 1.78 cm^{-1} separation. Below: Normal absorption. Above: Stark difference signal above with E = 19,000 volts/cm and signal polarity indicated.

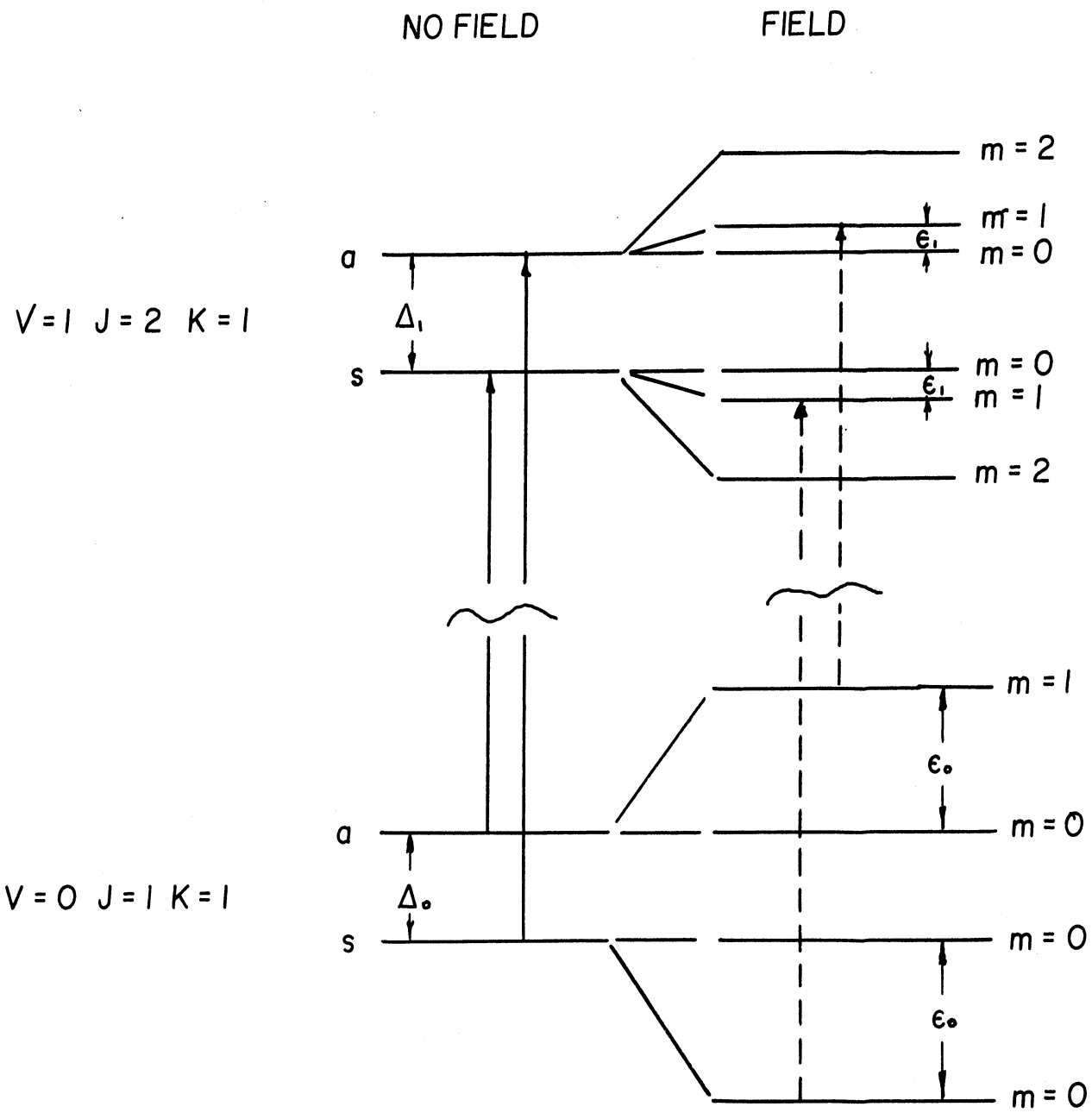

Fig. 24. Ammonia energy levels with and without electric field showing the usual allowed transitions (solid lines) and the parallel-polarized transitions (dashed lines) resulting from breakdown of the $s \leftrightarrow a$ selection rule in an electric field.

This information has already been obtained for NH_3 from a combination of microwave and infrared data, but the electric-field method would appear to be fruitful for cases of inversion splitting not already investigated that are more difficult to analyze because of their lack of symmetry—such as NH_2D, ND_2H, CH_3NH_2, etc.

4. H_2O.—A rather cursory examination was made of the Stark difference signals arising in the ν_1 and ν_3 O-H stretching fundamentals of H_2O to see the effects in a quite asymmetric top molecule. A 10,000 volt/cm square wave field acted on 1-cm pressure of H_2O in the cell. However, the optical path at the tungsten lamp source was not flushed long enough to remove the last traces of H_2O vapor, so that an appreciable amount of absorption at the more intense transitions was external to the Stark cell. A representative portion of the spectra, both normal and modulated by the electric field, is shown in Fig. 25. It is apparent that only a few levels are appreciably influenced by the electric field. The transitions with the largest Stark signals are listed below.

Stark Intensity	Freq. in cm^{-1}	Rotational States		Vib.	I. R. Intensity
		Upper	Lower		
10.5	3880.07	5_{-1}	4_0	ν_3	8.0
9.5	3869.86	6_{-5}	5_{-4}	ν_3	10.0
4.3	3863.48	2_2	1_{-1}	ν_3	0.8
2.5	3871.65	5_{-1}	4_{-3}	ν_1	3.4
2.4	3973.98	5_{-1}	4_{-4}	ν_3	0.3
2.3	3779.78	1_{-1}	0	ν_3	10
2.2	3892.83	3_{-1}	2_{-2}	ν_3	0.5
2.2	3711.09	2_{-1}	1_{-1}	ν_1	40.0

The Stark intensity given above is the peak value of the difference signal, and should be considered as no more than a crude indication of the Stark effect, for the strong lines are in a nonlinear absorption range, and also the water vapor absorption outside of the cell will further distort the apparent size of the difference signal. One would expect that the low J states of an asymmetric rotor would show the largest Stark shifts. The fact that the strongest signals are associated with higher J terms indicates the presence of a interacting nearly degenerate pair of levels. Golden and Wilson[15] give as the necessary condition for the two levels to be perturbed by an electric field, a nonvanishing value of the matrix element of the permanent dipole moment connecting the states, or hence that the transition between the levels is an allowed one in the pure rotation spectrum. Only two pairs of such levels occur in the ground state with a separation of less than 10 cm^{-1} up to $J = 8$. These are 6_{-5} and 5_{-1} separated by 1.06 cm^{-1} and 3_{-2} and 2_{+2} separated by 6.18 cm^{-1}. The fact that one or the

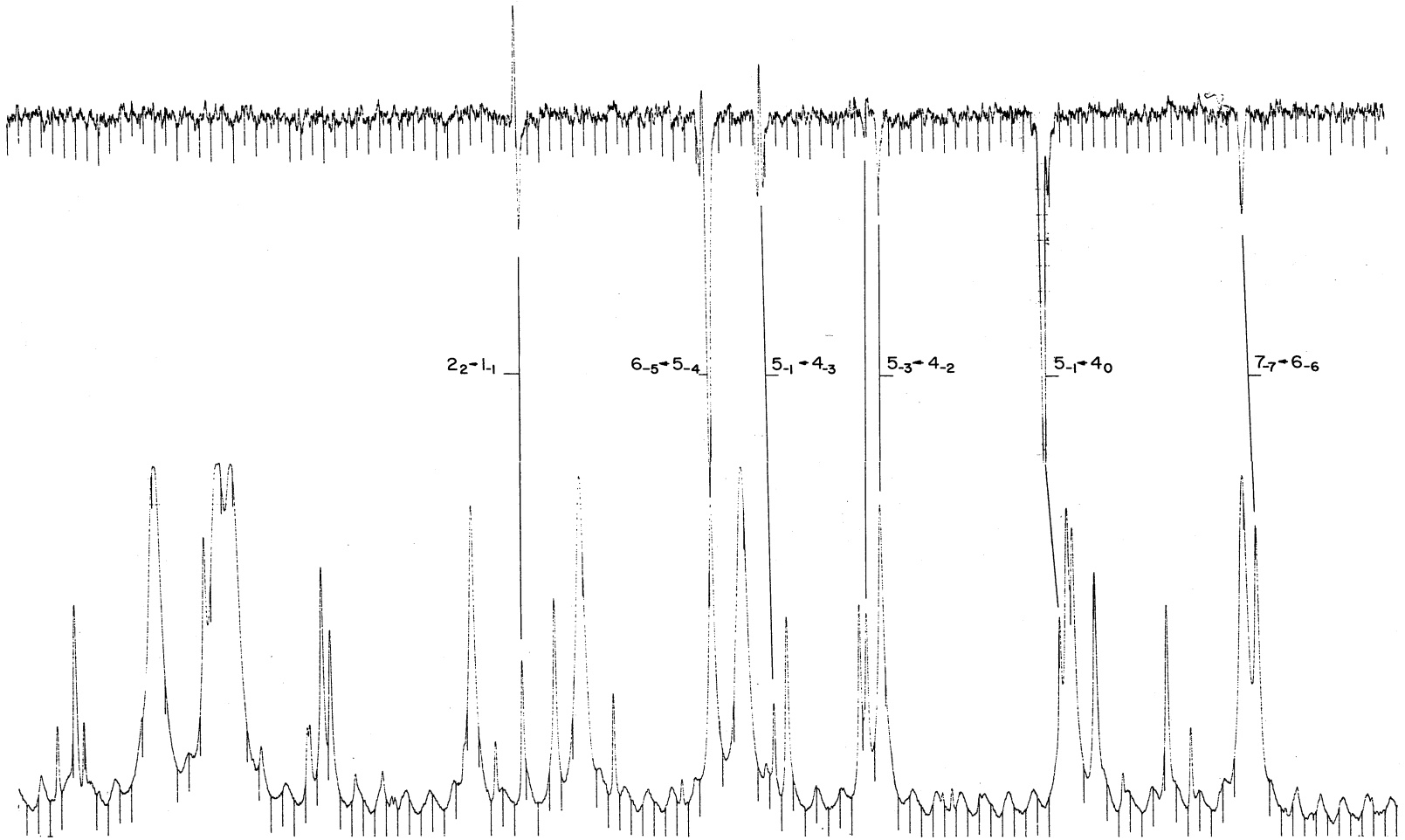

Fig. 25. Below: Normal absorption of water vapor near 3870 cm^{-1}, 1 cm pressure. Above: Stark difference signal, 10^4 volts/cm with transitions indicated.

other of these levels is involved in the five largest Stark effects gives strong support to this view. The extensive work necessary to calculate the Stark shifts of H_2O does not appear to be justified at the present time. It is hoped, however, to study several other molecules having a permanent dipole moment along the A or C axis (as H_2CO) rather than the B axis (as H_2O) since near degenerate interacting pairs of rotational levels occur regularly for each J value.

REFERENCES

1. P. Jacquinot, J. Opt. Soc. Am. 44, 761 (1954).

2. Kline, Ph.D. thesis, Purdue Univ. (1952).

3. A. E. Martin, Nature 180, 231 (1957).

4. P. Giacomo and P. Jacquinot, J. Phys. et Radium 13, 59A (1952).

5. C. S. French and A. B. Church, Carnegie Inst. of Wash. Ann. Rept. 162 (1955).

6. J. P. Pemsler, Rev. Sci. Inst. 28, 274 (1957).

7. J. D. Hardy, Phys. Rev. 38, 2162 (1931).

8. Giguère, Can. J. Chem. 33, 527 (1955).

9. Massey and Bianco, J. Chem. Phys. 22, 442 (1954).

10. Massey and Hart, J. Chem. Phys. 23, 942 (1955).

11. Randall and Firestone, Rev. Sci. Inst. 9, 404 (1938).

12. Stark, Berl. Akad. Wiss. 40, 932 (1913).

13. R. W. Terhune and C. W. Peters, J. Mol. Spect. 3, 138 (1959).

14. Kusch and Hughes, Handbuch der Physik XXXVII/1, 141, Springer.

15. Golden and Wilson, J. Chem. Phys. 16, 669 (1948).

UNIVERSITY OF MICHIGAN
3 9015 02827 4630